INVESTIGATING THE EASTERN EXTENT OF THE SEATTLE FAULT ZONE THROUGH DEPTH TO BEDROCK AND BOREHOLE ANALYSIS IN BELLEVUE, WA

Bryan W. Holmes

A report prepared in partial fulfillment of
the requirements for the degree of

Master of Science
Earth and Space Sciences: Applied Geosciences

University of Washington

November 2014

Project mentor:
Brian Sherrod, U.S. Geological Survey

Internship coordinator:
Kathy Troost, University of Washington, Troost Geosciences, Inc.

Reading committee:
Juliet Crider, University of Washington
Steven Walters, University of Washington

MESSAGe Technical Report Number: [013]

ABSTRACT

This study identifies lineaments that indicate fault activity and strengthens previous interpretations of structures within the eastern extent of the Seattle Fault zone in Bellevue, WA. My investigation has compiled geotechnical subsurface data, high-resolution LiDAR imagery, and ground-penetrating radar to produce strip log sections transecting identified lineaments and depth-to-bedrock maps exposing fault structure. My work incorporates field investigation, multiple publicly available datasets, and subsurface modeling. My results include a map showing twenty-eight identified surface lineaments, five strip-log sections, and interpolated depth-to-bedrock and minimum-depth-to-bedrock maps. Several lineaments identified in the minimum-depth-to-bedrock raster are parallel to the Seattle Fault zone and suggest the presence of small splay faults beneath east Bellevue. These results strengthen previous interpretations of seismic profile data located in the study area. Another lineament identified in the minimum-depth-to-bedrock raster suggest an unmapped tear fault accommodating differential offset along fault strike between Mercer Island and Bellevue. This work also demonstrates the utility of publicly available datasets such as geotechnical subsurface explorations and LiDAR imagery in supplementing geologic investigations in the eastern extent of the Seattle Fault zone.

ACKNOWLEDGEMENTS

I would like to give thanks to those who have made this project possible: Kathy Troost for project inspiration, guidance, and local expertise; Brian Sherrod, U.S. Geological Survey, for his mentorship and expertise; Sue Bednarz and Jacobs Associates for supplying relevant geotechnical boring logs; Matthew Benson, Golder Associates, and Northwest Geophysics for their expertise in geophysics and GPR survey equipment; Mike Brown for assistance with geophysical interpretation; Steven Walters for GIS expertise; Juliet Crider for her structural geology expertise and guidance on research methods and writing; and Rebekah Cesmat and John Manke for their collaboration.

TABLE OF CONTENTS

LIST OF FIGURES

LIST OF TABLES

1. INTRODUCTION

Seismic hazards in the greater Seattle area have been investigated extensively using the techniques of stratigraphy, geophysics, paleoseismology, and geomorphology, among other techniques (Johnson et al., 1994, 1999; Pratt et al., 1997; Wells et al., 1998; Atwater, 1999; Blakely et al., 2002; Sherrod, 2002; Haugerud et al., 2003; Nelson et al., 2003; Brocher et al., 2004; McCaffrey et al., 2007; Kelsey et al., 2008; Liberty and Pratt, 2008; Nelson et al., 2014). The specific seismic hazards resulting from activity of crustal faults in the greater Seattle area and throughout the Puget Lowland remain poorly constrained due to uncertainty in the location, structure, behavior, and timing of fault related events (Liberty and Pratt, 2008). These events pose a serious threat to lives and infrastructure in the increasingly urbanized Puget Lowland. In particular, the Seattle Fault is a known seismic hazard lying beneath two of the state's most densely populated cities, Seattle and Bellevue (Gower et al., 1985; Bucknam et al., 1992).

This study aims to investigate the location and structure associated with strands of the Seattle Fault near its eastern extent in Bellevue, WA. I use available high-resolution LiDAR imagery, geotechnical subsurface logs, ground-penetrating radar surveys, digital data analysis, and subsurface modeling.

Geologic investigations in the Puget Lowland face many challenges due to the region's urban development, forested terrain, and glacial history. Dense development in major urban centers has removed and obscured surficial features that are critical for interpreting the geomorphology. Development in some areas can mask bedrock outcrop. Also, field studies in developed areas must carefully avoid traffic and respect private property. Pacific Northwest temperate forests surrounding and interspersed within these urban centers also play a role in masking bedrock exposure and attenuating geomorphic features.

Repeated glaciation in the Puget Lowland has led to a complicated layering of glacial and nonglacial deposits overlying existing bedrock topography (Troost and Booth, 2008). It is commonly difficult to distinguish these deposits in the field, and even more difficult to correlate them laterally. This study attempts to overcome these challenges by making use of a variety of subsurface data, combined with published geophysical data and analysis of LiDAR-derived topographic data.

2. SCOPE OF WORK

This study investigated the subsurface geology underlying Bellevue, WA, near the eastern extent of the Seattle Fault (Fig. 1). The work involved field reconnaissance and background research, gathering data, analysis of LiDAR and borehole data, field surveying with ground-penetrating radar, interpretation of results, and reconstruction of existing depth-to-bedrock and geologic maps. Field reconnaissance included making observations of bedrock exposures in Bellevue to become familiar with the lithology of units and looking for evidence of fault deformation. Background research was focused on the structure of the Seattle Fault and depth to bedrock, particularly in the Bellevue area. LiDAR imagery and borehole data was analyzed using ArcGIS and RockWorks software. Ground-penetrating radar surveys were performed where lineaments or offsets have been observed in the topography and subsurface data. Results are displayed using strip log cross-sections, interpolated raster images, and reconstructed depth-to-bedrock maps.

3. GEOLOGIC SETTING

Oblique subduction of the Juan de Fuca plate along the continental margin, interacting with clockwise rotation of crustal blocks in the Cascadia Forearc, is accommodated by north-south shortening in the Puget Lowland (Pratt et al., 1997; Wells et al., 1998). This shortening is expressed as a series of east-west and northwest-southeast trending active faults, producing a series of basins and uplifts within the Puget Lowland (Snavely and Wells, 1996; Pratt et al., 1997; Wells et al., 1998; Liberty and Pratt, 2008). The Puget Lowland is a broad valley in Washington State, located between the Cascade Range and Olympic Mountains Coast Range (Fig. 2). The Seattle Fault zone is an area of east-trending, north-verging thrust faults and related strands extending across the Puget Lowland (Fig. 3). The fault has displaced Eocene basement rock northward relative to the structurally-bound Seattle sedimentary basin to the north (Johnson et al., 1994).

Glacial and glacio-fluvial infill deposits found at varying elevations in the Puget Lowland suggest that a significant amount of isostatic rebound and/or tectonic deformation has occurred since the last glacial maximum ~14 kya (Thorson, 1980; Booth, 1994). These deposits include advance outwash, till, glacial lacustrine clays, and recessional outwash. Deposition of these units over existing bedrock topography, reworking of sediments from repeated glacial advance and retreat, and compaction of both nonglacial and glacial sediments all lead to a complicated stratigraphic record. Within the study region, bedrock units are exposed at the surface in areas south of Bellevue while the remaining majority of exposed geology consists of Quaternary alluvium, interglacial deposits, and glacial deposits.

4. PREVIOUS WORK

The Cenozoic tectonic history of the Puget Lowland in Washington State remains poorly understood because of thick (~9-10 km) overlying Quaternary deposits in the Seattle basin and the submergence of features underneath Puget Sound (Johnson et al., 1994). Geophysical and aeromagnetic surveys have provided valuable information constraining the location of the Seattle Fault and its strands (Pratt et al., 1997; Johnson et al., 1999; Nelson et al., 2003; Liberty and Pratt, 2008), but the geometry and deformation of the subsurface geology is still a major topic of debate. Although there is general consensus that the Seattle Fault is a north-directed thrust fault, it is also clear that there is not a single fault surface, and the specific geometry of fault strands within the fault zone is not well defined. Johnson et al. (1994) concluded that the Seattle fault is a contractional zone and that flexure of the Seattle basin is caused by the crustal load placed on its southern margin by uplifted Crescent Formation bedrock. Pratt et al. (1997) proposed a wedge model for the Seattle fault, where a slab of Crescent Formation basalts was ramped over deeper material, resulting in regional uplift. Johnson et al. (1999) define the leading edge of the fault, describe two main segments divided by an active north-trending strike-slip fault zone, and estimate the maximum age for initiation of the Seattle fault's northernmost strand to be no older than ~10 Ma. Liberty and Pratt (2008) suggest a fault-propagation fold model for the Seattle Fault, which includes a blind fault tip beneath the deformation front, a forelimb breakthrough, and a large backthrust. Each of these models makes different interpretations of the subsurface geometry of the fault zone. Interpretation of the subsurface conditions is critical for understanding crustal deformation associated with the active fault and for estimating earthquake hazards in the densely populated cities of Seattle and Bellevue. This work aims to contribute to that effort.

Because the Seattle Fault is a major thrust zone displacing bedrock over glacial and interglacial sediments, depth to bedrock may be one of the most robust ways to locate the fault and its strands. Yount et al. (1985) produced a depth-to-bedrock map of the Seattle 30' by 60' Quadrangle that shows bedrock at and near the surface south of Bellevue and quickly dropping to greater than 200 feet toward the north and northwest. Their map was developed using subsurface logs, but these were sparsely located throughout the map area with a majority of the logs sourced from water wells. Part of my investigation aims to improve upon the depth-to-bedrock mapping in the Bellevue study area by incorporating a larger, more reliable subsurface dataset from geotechnical borings.

Digital modeling of the Puget Lowland landscape using LiDAR has aided in identification of fault scarps in the Seattle fault zone (e.g. Haugerud et al., 2003; Nelson et al., 2003). Many of these fault scarps have been trenched and provide evidence of large, Holocene, surface-rupturing earthquakes (Sherrod et al., 2000; Sherrod, 2002; Nelson et al., 2003). Trenching for deposits that date fault activity can help reduce the uncertainty in evaluating earthquake hazards in the Puget Lowland. Particularly relevant to my study, excavation at two sites near Vasa Park on the west shore of Lake Sammamish (within the city of Bellevue) expose Holocene fault rupture at contacts between Quaternary glacial deposits and Miocene bedrock (Sherrod, 2002).

5. METHODS AND ASSUMPTIONS

Here I outline the processes of data collection and analysis, and review the assumptions made in undertaking this study. The general workflow was to first compile the LiDAR and subsurface data in ArcGIS, filter the subsurface boreholes within the study area, and then export the borehole data into RockWorks modeling software. In RockWorks, I build strip log sections and organize a dataset for interpolating bedrock surfaces at depth. Interpolation in ArcGIS led to the creation of rasterized images showing depth- and minimum-depth-to-bedrock. Site selection for the ground-penetrating radar surveys was based on identified lineaments from the LiDAR and places with bedrock offset found in the subsurface models. Results were compared with geophysical data collected from previous studies.

5.1 Data Sources

The two principal data sources for this study are the Puget Sound LiDAR Consortium (http://pugetsoundlidar.ess.washington.edu/) and the GeoMapNW project (http://geomapnw.ess.washington.edu/). LiDAR imagery of the Seattle Fault zone, extending from east of Lake Sammamish to Puget Sound, was downloaded from the Puget Sound LiDAR Consortium website as a set of 30 raster tiles (Puget Sound LiDAR Consortium, 2014). These rasters were merged and processed to be displayed as a colorized raster and a hillshade raster. This digital elevation model (DEM) provides the basemap for displaying the results of analysis. Geotechnical subsurface data for the Greater Seattle area (Fig. 4) was compiled by the GeoMapNW project and made available on the Washington State Department of Natural Resources Subsurface Geology Information System (Department of Natural Resources, 2014). In order to efficiently query the subsurface data, we obtained an original copy of the GeoMapNW dataset from director Kathy Troost (*personal communication*, 2014). This data can be imported into an ArcGIS file geodatabase and queried for certain attributes. Nine additional borehole logs were obtained from Jacobs Associates, a global consulting agency specializing in tunnel engineering, who consulted with King County about the feasibility of tunnel alternatives for wastewater management in Bellevue.

5.2 ArcGIS Analysis

My first step in analysis of the data was to visually scan the DEM for linear or scarp-like features. In a preliminary GIS analysis, my goal was to identify east-west trending steep slopes or topographic inflections because these may indicate the presence of north- or south-verging fault strands typical of the Seattle Fault zone. These lineaments may coincide with apparent stream knickpoints, which appear in the DEM as sharp turns in the stream path. Using the slope and aspect tools in ArcMap, I was able to reclassify the DEM to show only slopes with northerly or southerly aspects and steepness greater than twelve degrees. Using this reclassified raster as an aid, twenty-eight lineaments were identified in my study area (Figure 5).

Exploration points from the subsurface dataset were imported into ArcMap and clipped to the study area. Two of the borehole logs (BH-1 and BH-6) from Jacobs Associates that are located within my study area were manually entered into a spreadsheet and added to the subsurface dataset in ArcGIS. Exploration points were displayed using symbols sized proportionally to the total depth of exploration (Figure 6). Each exploration point has an identification number (EXPLOR_ID) that relates to a table of layer data from the exploration logs. The two columns that were used to filter the exploration layer table are *Major Material* and *Material Log Unit*. *Major Material* is the primary lithology present in each logged layer (Table 1). *Material Log Unit* refers to the specific stratigraphic or lithologic unit name assigned by the core logger. The subsurface layer table was searched for layers with either sedimentary bedrock listed as *Major Material* or any bedrock unit listed as *Material Log Unit.* Weathered bedrock units were included. Out of a total of 7,243 exploration points within the study area, 755 points contain bedrock layers.

5.3 RockWorks Analysis

RockWorks is a computer modeling program used by the mining, petroleum, and environmental industry for subsurface visualization (RockWare, 2014). RockWorks was chosen for this study for its borehole database management and modeling capabilities. The analysis of borehole data in RockWorks includes producing borehole transects, calculating a depth-to-bedrock and minimum-depth-to-bedrock attribute, and interpolating a surface representing the sediment-bedrock contact underlying Bellevue. Several RockWorks import spreadsheets had to be filled in with the filtered borehole data from ArcGIS. These spreadsheets provided information on the location and depth of boreholes, the lithologies in each borehole, the variety of lithology types, any interpreted stratigraphy in the borehole logs, and the variety of stratigraphy types. Elevation information for each borehole was extracted from the DEM.

Strip log sections were created for several key areas: Sunset Ravine, Somerset Hill, and the Lake Washington shoreline (Figure 7). These strip log sections were selected to cross interesting geomorphic features and in areas where there is sufficient data. Sunset Ravine trends north-south across an identified lineament just south of Interstate-90, toward the northern boundary of the deformation zone. Field exposures at Sunset Ravine show evidence of offset within lacustrine sediments. Somerset Hill has three identified east-west lineaments and a deep, well-documented boring (BH-6). A north-trending series of deep borings located less than half of a mile from the Lake Washington shoreline were sourced from a single tunnel project funded by King County Transportation. These borings were selected for their consistency in depth and quality of logging. Strip log sections created by RockWorks are displayed poorly, so each section was refined using Adobe Illustrator.

In order to interpolate a bedrock surface, I duplicated the RockWorks spreadsheet and consolidated the lithology. Any layer described as bedrock was relabeled "Bedrock," while all other layers were relabeled "Sediment." A "depth-to-bedrock" column was added to the spreadsheet and calculated by taking the difference between boring elevation and bedrock top. Initially, a RockWorks grid model was created from the relabeled borehole data using an inverse distance weighted interpolation method. The resulting grid model was poorly contoured and did not show reasonable geology. I instead exported the data back to ArcGIS and generated an interpolated raster using the ordinary kriging method with a spherical model. Ordinary kriging is commonly used in this context because it provides the best linear unbiased estimates and assumes no spatial trend in the data (Chung and Rogers, 2012).

In order to make use of more of the existing subsurface data in my study area, I incorporated exploration points greater than 30 feet deep in my study area that did not intercept a bedrock layer to create a minimum-depth-to-bedrock model. The new model interpolated a surface using the bottom of the "Sediment" layer instead of the top of the "Bedrock" layer. The resulting rasterized image displayed greater detail where bedrock borings were sparse in the study area.

5.4 Ground-penetrating radar survey

The ground-penetrating radar (GPR) surveys were performed with assistance from project collaborators Rebekah Cesmat and John Manke. The GPR equipment was loaned to us from Northwest Geophysics owner Matthew Benson. We were provided with the Mala GroundExplorer system, GX 80-MHz antenna, and RadExplorer software. The antenna had an attached survey wheel and data were collected at 0.5-inch intervals.

Four sites were selected for GPR surveying in the study area. The sites were selected by their concurrence with identified lineaments and borehole transects, and also by their accessibility. The site at Sunset Ravine is an unpaved walking trail that parallels the creek along the east crest of the ravine. There are two observable topographic inflections sloping toward the north along the unpaved trail, which were targeted in the survey. The transect on Somerset Hill is a residential street (140th Ave SE) that mostly courses north-south and intersects the location of the BH-6 borehole from Jacobs Associates. Borehole data on Somerset Hill indicates bedrock depths ranging from 5 to 19 feet, which is in the depth range of the GPR equipment. The other two sites are approximately parallel to the series of near-shoreline borings; the first is on an unpaved trail following a creek between SE 60th Street and 113th Place SE, and the second is in an open field west of Chinook Middle School.

GPR data were processed and analyzed using RadExplorer v1.4 software. A series of standard processing steps was applied to the data (Matthew Benson, *personal communication*). These processing steps included the following: DC removal, background removal, time-zero adjustment, amplitude correction, bandpass filtering, and velocity analysis. A topographic correction was made to all but seven of the GPR profiles surveyed by John Manke, Rebekah Cesmat, and myself.

5.5 Assumptions

During the process of searching for lineaments, I assumed that scarp-related features were oriented generally east-west (based on our current understanding of the structure of the fault zone as a system of north-verging thrusts and north-dipping backthrusts) and well preserved despite urban development. For the borehole data analysis, I assumed that each exploration was accurately logged and that documented stratigraphic interpretations were based on evidence. Interpolated models of depth to bedrock assumed no spatial trends and a continuous sediment-bedrock contact.

6. RESULTS

The twenty-eight lineaments identified in the study area are shown in Figure 5, over the DEM and LiDAR hillshade basemap. Several of these lineaments coincide with those identified by my collaborators Rebekah Cesmat and John Manke. The lineaments extend from the western shore of Mercer Island to Lakemont Highlands in Bellevue, and from Lake Boren to Interstate 90. The lineaments are mostly straight lines, ranging in length from about 750 to 5,130 feet, and have a mean orientation of about 98 degrees east of north. Individual orientations follow previously mapped lineaments in the study area. Seven of the lineaments correspond to stream valleys, four transect hills in Bellevue, and the remaining are simply scarp-like features. Some of these lineaments, including those corresponding to stream valleys, may be related to fault activity. East-west trending lineaments in this area may also result from east or west slope drainages on north-south trending drumlin features.

The subsurface data within the study area is shown in Figure 6, symbolized to show total depth. Noticeable trends in this figure include deep borings following the path of Interstate 405, Interstate 90, and Lakemont Boulevard SE, shallow to medium depth borings densely distributed along shoreline real estate on Mercer Island, dense borings following stream beds, and shallow borings in neighborhood developments. Deep borings in my study area appear to be related to highway construction and tunnel projects, which helps explain their distribution and scarcity. Overall, the density and distribution of subsurface logs in this area is much greater than what was available in previous studies. Yount et al. (1985) created a depth-to-bedrock contour map that included this study area, but their subsurface logs were limited to twenty-one water wells, only nine of which intercepted bedrock. Despite the greater overall density of subsurface logs, the challenge of finding a sufficient number of deep borings that transect possible fault-related lineaments remains.

6.1 Strip Log Sections

Figures 8 through 10, 12, and 13 show the strip log sections created for the three key areas (Somerset Hill, Sunset Ravine, and Lake Washington shoreline). Each section contains borings of varying depths, most of which include glacially-derived sediments.

The Lake Washington shoreline section shows discontinuous layers of sand, silt, and clay, below the surface profile (Fig. 8). A thick unit of sand visible in borings 88239 and 88237 does not carry over in surrounding borings 88234 and 88235. Clay units appear in nine of the twelve borings. The clay found in boring 88233 is laminated and dipping 70 degrees. The clay units are very likely glacial lacustrine clays, which are typically bounded by an advance outwash sand below and a recessional outwash sand above. This stratigraphic relationship is most clearly seen in boring 88233. Steeply dipping lamination in this clay unit may be related to landsliding, glacio-tectonic deformation, or fault uplift. The strip log section shows units thinning or pinching. This apparent thinning may simply be a result of deposition over existing topography, erosion from the overriding glacier, or may indicate fault offset. Bedding information would help confirm fault offset through these sediments, but the majority of the borings have no bedding information or lack bedding orientations.

The two Somerset Hill sections show bedrock near the surface, following the topography (Figs. 9 and 10). Borings 86049 and 86047 contain bedrock layers that were logged as weathered silty sandstones, with no reported bedding or fracturing. BH-6 is a recently drilled, 735 feet deep boring that shows silt- and sandstones of the Blakely Formation beginning at a depth of 19 feet. A majority of these sedimentary layers in BH-6 displayed moderate to intense fracturing and a few included bedding information. Increased fracturing may indicate a nearby fault strand, where material experiences a greater degree of deformation and shear stress. The amount of fracturing in BH-6 may correlate to the lineament identified just to the north. A seismic reflection profile taken from Liberty and Pratt shows predominantly north-dipping strata parallel to the Somerset Hill transects and less than a half mile to the west (Fig. 11). By comparing the two results, we can make a stronger interpretation of the BH-6 strip log section and suggest that it shows a north-dipping bedrock bedding surface approaching a fault strand.

The Sunset Ravine sections consist of glacial and nonglacial sediments, with several layers interpreted as till or outwash (Figs. 12 and 13). The strip log section in Figure 12 utilizes borings that are detailed enough to display some interpreted glacial stratigraphy and a compaction surface, but fail to show significant offset within Quaternary sediments.

6.2 Depth-to-Bedrock Maps

A portion of Yount et al. (1985) depth-to-bedrock map is shown in Figure 14. My new depth-to-bedrock map shows bedrock at or near the surface in the southeast corner of the study area (Fig. 15). The detail in this corner of the map is much better than in the west half of the map because of the density of bedrock borings. The visible trend shown in the depth-to-bedrock map is that the sediment-bedrock contact drops off toward the north and northwest.

The minimum-depth-to-bedrock map shows greater raster detail because more borings were incorporated in the interpolation process (Fig. 16). The minimum-depth-to-bedrock map shows both the bottom depth of sediment overlying bedrock and the bottom depth of 30-foot borings that do not reach bedrock. For identifying fault strands, this may be helpful in areas where bedrock borings are dense but potentially misleading in areas that only represent the bottom depth of borings that do not reach bedrock.

6.3 GPR Profile

The Sunset Ravine GPR profile shows a prominent planar reflector at a depth between three and four meters, near the northern end of the profile (Fig. 17). A planar reflection can result from a strong contrast between soil horizons, the water table, a compaction surface, or a change in lithology (van Overmeeren, 1998). Since this reflective surface roughly follows topography, it is likely controlled by a lithologic change, rather than the water table. The strip log section at Sunset Ravine contains borings that describe a compaction surface at a definable depth (Fig. 12). I interpret the identified GPR reflector to represent that compaction surface within Quaternary sediments.

Interference from roots and street infrastructure in the other three sites produced noisy GPR images, and these data are not included in this report.

7. DISCUSSION

For this study, identification of lineaments is intended to provide focus in the analysis of borehole data and GPR surveying. Lineaments may be related to several processes, including: stream incision, landsliding processes, urban development, differential weathering due to abrupt changes in lithology, or fault rupture. The lineaments identified within the study area appear to be related to either stream incision, changes in lithology, or fault rupture. At the surface, a change in lithology or location of a stream channel may both be directly the result of faulting for these two reasons: displacement of lithologic units and weakening of material through fracturing. Analysis of the subsurface data may reduce this uncertainty either by showing offset in lithology between two adjacent borings or by providing evidence of increased fracturing.

The broad goal of this study is to assess the potential of utilizing geotechnical borehole data in a subsurface investigation of earthquake hazards related to surface-breaking faults. The subsurface geotechnical information, while extensive, has important limitations. Many adjacent borings containing bedrock in this study area are shallow and have very little information about the nature of the bedrock unit. Increased fracturing was observed in both

BH-1 and BH-6 borings, but the interpretation of "increased fracturing" may in fact simply emerge because neighboring borings having relatively cursory log data. It is possible to interpret a bedrock surface for the strip log sections on Somerset Hill, but the boring logs are not detailed enough to say whether the interpreted surface is a bedding plane, an erosional surface, or if it is cross-cut by unconformities.

The GPR survey provided complimentary near-surface data that gave us a better understanding of the nature of material between adjacent borings at one site.

The depth-to-bedrock map (Fig. 15) appears to show better contour detail in the southeast corner than the map (Fig. 14) produced by Yount et al. (1985) but does not accurately portray depth to bedrock in the rest of the map area. A few anomalous zones in the west half of the map can be explained by the lack of boring density in those areas or by possible inaccuracy of core logging. The general trend shown by the depth-to-bedrock map matches that of Yount et al. (1985) in that bedrock near or at the surface in the southwest corner quickly drops off toward the north and northwest. This trend is consistent with structural models showing the sediment-bedrock contact dropping quickly from south to north (Nelson et al., 2014).

The minimum-depth-to-bedrock map (Fig. 16) shows bedrock close to the surface in the southeast corner that quickly drops off to north and west. It is unlikely that the west half of the map accurately displays this minimum depth, because most of the borings on Mercer Island are too shallow to reveal the bedrock depth suggested by geophysical surveys (Johnson et al., 1999; Blakely et al., 2002). Several lineaments identified from the interpolated minimum-depth-to-bedrock in the map area may reveal fault-related geometry (Fig. 18). These were visually identified as areas where changes in depth to bedrock were linearly consistent, depth contours were closer together, and the change was at least 30 feet. The east-west trending lineament to the north of Somerset Hill is situated where bedrock strata begin to dip prominently to the north (Fig. 11), as observed in published seismic reflection profiles (Liberty and Pratt, 2008). The map does not accurately portray the large change in depth of this north-dipping bedrock surface because of the lack of deep borings in the northern extent of the study area. However, the orientation and location of this lineament matches what we would expect in this area of the fault zone. This prominent bedrock lineament may be the eastern expression of the Seattle monocline suggested by previous studies (Johnson et al., 1999; Brocher et al., 2004; Kelsey et al., 2008; Liberty and Pratt, 2008). The interpolation of depth to bedrock from borings is unable to expose the underlying geometry of the monocline or confirm the hypothesized blind-tip of the fault-bend fold geometry, but is able to provide a spatial constraint on the hinge of the monocline.

Two east-west trending lineaments located south of Somerset Hill connect two prominent lows in the sediment-bedrock contact (Fig. 18). These lineaments may indicate other north-verging faults or antithetic backthrusts off the main trace of the fault. Liberty and Pratt (2008) suggest a backthrust off of the Vasa Park strand that extends to the surface at the location of this lineament. Their structural interpretation suggests an uplifted block between the Vasa Park strand and the antithetic backthrust, which causes bedrock to be nearer the surface closer to the middle. The borings located between the east-west trending lineaments in Figure 18 indicate that depth-to-bedrock is shallower toward the center. While the borings do not directly give evidence of fault offset in this part of the study area, the interpolation appears to strengthen the structural interpretation made by Liberty and Pratt (Fig. 19).

The western extent of two of the east-west lineaments identified in the minimum-depth-to-bedrock map are problematic in that they are abruptly cut by a north-northeast trending lineament that divides the study area (Fig. 18). This pronounced feature indicates a steep change in depth to bedrock, dropping nearly 200 feet from east to west over a distance as short as ~500 feet. An abrupt change in bedrock depth may be attributed to poor digital contouring, paleotopography beneath Quaternary deposits, differential offset along fault strike, or an unmapped tear fault working to accommodate differential offset. Intense fracturing within Blakely Formation silt- and sandstones, observed in Jacobs Associates BH-1 boring on the east side of the lineament, suggests the possibility of fault activity. Another explanation for fracturing and erosion of bedrock at this location is that glacio-tectonic forces and glacio-fluvial erosion may have been amplified in discrete zones across the fault zone, creating a range of erosion and slip rates. Investigation of the area using deep subsurface geophysical survey techniques is necessary to further define the extent and nature of this lineament.

8. CONCLUSION AND RECOMMENDATIONS

My investigation of the structure of the Seattle fault under Bellevue has led to the compilation of multiple sources of relevant, geotechnical subsurface data to produce strip log sections through lineaments identified within the fault zone, depth-to-bedrock maps of the study area that expose fault structure, and further confirmation of fault geometry interpreted from geophysical profiles. Given the availability of a high-resolution digital elevation model (such as LiDAR), surface breaks relating to fault structure are identifiable and can be analyzed through borehole modeling. Geotechnical data from varying dates and sources are difficult to interpret as a whole because of their emphasis on material strength properties, their typically small depths, and lack of bedding orientation information. Collection of GPR data is complicated by electromagnetic interference from urban infrastructure. Combining borehole analysis with existing geophysical profiles helps strengthen interpretations by providing lithologic constraints. Depth-to-bedrock maps derived from an interpolation of borehole data may identify discrete structures, which I interpret to be of fault-origin.

This investigation has provided a new understanding of the fault structure beneath Bellevue, Washington. Geotechnical boring logs provide a bedrock depth that can be correlated with geophysical data. One key finding of this study is that Liberty and Pratt's (2008) interpreted uplift block, lying between the Vasa Park strand of the Seattle fault and a north-dipping backthrust, is supported by evidence from geotechnical boring logs. In addition, the block is abruptly truncated at the western edge by a previously unmapped, structural or glacio-erosional feature that divides the study area into two distinct zones.

Well-documented boring logs proved useful in this study in helping to interpret identified structures. For future geotechnical exploration of the subsurface, it is clearly important to log thoroughly while taking into account local glacial history and fault hazards. I strongly recommended that any investigation of subsurface geometry, in a faulted urban setting, should incorporate available geotechnical datasets to strengthen their interpretation of otherwise potentially enigmatic structures. Further work for this study should complete seismic profiles transecting the north-trending lineament identified as a potential tear fault and expand the interpolation of bedrock borings to a regional scope that encompasses the Greater Seattle area.

9. LIMITATIONS

The limiting aspects of this study develop as a consequence of using a variety of existing data, in a repeatedly glaciated environment, to look at concealed fault structures underlying an urban setting. The dataset of subsurface explorations contained borings, test pits, water wells, and excavations (Table 2). These different methods of exploration are carried out for distinct purposes, with different logging techniques, each with their own limitations. The borehole data in my study area displayed a critical lack of stratigraphic interpretation and bedrock bedding information. Some of this data was documented as early as the 1930s and 1940s, and over one third of the data has low to medium location confidence. The depth-to-bedrock results are limited by their interpolation method and the amount of bedrock data within the study area.

REFERENCES

Atwater, B. F., 1999. Radiocarbon dating of a Seattle earthquake to AD 900–930. *Seismological Research Letters*, Vol. 70, No. 2, p. 232.

Blakely, R. J., Wells, R. E., Weaver, C. S., Johnson, S. Y., 2002. Location, structure, and seismicity of the Seattle Fault Zone Washington: Evidence from aeromagnetic anomalies, geologic mapping, and seismic reflection data. *Geological Society of America Bulletin*, Vol. 114, No. 2, pp. 169-177.

Booth, D. B., Troost, K. G., in preparation, Geologic map of the Mercer Island and Issaquah 7.5-minute quadrangles, Washington, *U.S. Geological Survey Scientific Investigations Map*.

Brocher, T. M., Blakely, R. J., Wells, R. E., 2004. Interpretation of the Seattle Uplift, Washington, as a passive-roof duplex. *Bulletin of the Seismological Society of America*, Vol. 94, No. 4, pp. 1379-1401.

Bucknam, R. C., Hemphill-Haley, E., Leopold, E. B., 1992. Abrupt uplift within the past 1700 years at southern Puget Sound, Washington. *Science*, Vol. 258, No. 5088, pp. 1611-1614.

Chung, J. W., Rogers, J. D., 2012. Estimating the position and variability of buried bedrock surfaces in the St. Louis metro area. *Engineering Geology*, Vol. 126, pp. 37-45.

Clement, C. R., Pratt, T. L., Holmes, M. L., Sherrod, B. L., 2010. High-Resolution Seismic Reflection Imaging of Growth Folding and Shallow Faults beneath the Southern Puget Lowland, Washington State. *Bulletin of the Seismological Society of America*, Vol. 100, No. 4, pp. 1710-1723.

Department of Natural Resources, 2014. *Washington State Geologic Information Portal*: Electronic document, retrieved from http://www.dnr.wa.gov/ResearchScience/Topics/GeosciencesData/Pages/geology_portal.aspx

Gower, H. D., Yount, J. C., Crosson, R. S., 1985. Seismotectonic map of the Puget Sound region, Washington. *Department of the Interior, US Geological Survey*.

Haugerud, R. A., Harding, D. J., Johnson, S. Y., Harless, J. L., Weaver, C. S., Sherrod, B. L., 2003. High-resolution lidar topography of the Puget Lowland, Washington. *GSA Today*, Vol. 13, No. 6, pp. 4-10.

Johnson, S.Y., Potter, C.J., Armentrout, J.M., 1994. Origin and Evolution of the Seattle Fault and Seattle Basin, Washington. *Geology*, Vol. 22, No. 1, p. 71.

Johnson, S.Y., Dadisman, S.V., Childs, J.R., Stanley, W.D., 1999. Active Tectonics of the Seattle Fault and Central Puget Sound, Washington—Implications for Earthquake Hazards. *Geological Society of America Bulletin*, Vol. 111, No. 7, pp. 1042-1053.

Kelsey, H.M., Sherrod, B.L., Nelson, A.R., Brocher, T.M., 2008. Earthquakes generated from bedding-plane-parallel reverse faults above an active wedge thrust, Seattle fault zone. *Geological Society of America Bulletin*, Vol. 120, pp. 1581-1597.

Liberty, L.M., Pratt, T.L., 2008. Structure of the Eastern Seattle Fault Zone, Washington State: New Insights from Seismic Reflection Data. *Bulletin of the Seismological Society of America*, Vol. 98, No. 4, pp. 1681-1695.

McCaffrey, R., Qamar, A. I., King, R. W., Wells, R., Khazaradze, G., Williams, C. A., Zwick, P. C., 2007. Fault locking, block rotation and crustal deformation in the Pacific Northwest. *Geophysical Journal International*, Vol. 169, No. 3, pp. 1315-1340.

Nelson, A.R., Johnson, S.Y., Kelsey, H.M., Wells, R.E., Sherrod, B.L., Pezzopane, S.K., Bradley, L., Koehler, R.D. and Bucknam, R.C., 2003. Late Holocene earthquakes on the Toe Jam Hill fault, Seattle fault zone, Bainbridge Island, Washington. *Geological Society of America Bulletin*, Vol. 115, No. 11, pp. 1388-1403.

Nelson, A.R., Personius, S.F., Sherrod, B.L., Kelsey, H.M., Johnson, S.Y., Bradley, L., Wells, R.E., 2014. Diverse rupture modes for surface-deforming upper plate earthquakes in the southern Puget Lowland of Washington State. *Geosphere*, Vol. 10, No. 4, GES00967-1

Pratt, T.L., Johnson, S.Y., Potter, C.J., Stephenson, W., Finn, C., 1997. Seismic Reflection Images beneath Puget Sound, Western Washington State: The Puget Lowland Thrust Sheet Hypothesis. *Journal of Geophysical Research*, Vol. 102, No. B12, pp. 27469-27489.

Puget Sound LiDAR Consortium, 2014. *Data.* Retrieved from http://pugetsoundlidar.ess.washington.edu/lidardata/

Sherrod, B.L., Bucknam, R.C., Leopold, E.B., 2000. Holocene relative sea-level changes along the Seattle fault at Restoration Point, Washington. *Quaternary Research,* Vol. 54, pp. 384-393.

Sherrod, B.L., 2002. Late Quaternary Surface Rupture Along the Seattle Fault Zone Near Bellevue, Washington. *American Geophysical Union, Fall Meeting*, abstract #S21C-12.

Troost, K. G., Booth, D. B., 2008. Geology of Seattle and the Seattle area, Washington. *Reviews in Engineering Geology*, Vol. 20, pp. 1-36.

RockWare, 2014. *RockWorks*. Retrieved from https://www.rockware.com/product/overview.php?id=165

van Overmeeren, R.A., 1998. Radar facies of unconsolidated sediments in The Netherlands: A radar stratigraphy interpretation method for hydrogeology. *Journal of Applied Geophysics,* Vol. 40, pp. 1-18.

Wells, R.E., Weaver, C.S., Blakely, R.J., 1998. Fore-arc migration in Cascadia and its neotectonic significance. *Geology,* Vol. 26, pp. 759-762.

Yount, J.C., Dembroff, G.R., Barats, G.M., 1985, Map showing depth to bedrock in the Seattle 30’ by 60’ Quadrangle, Washington: *U.S. Geological Survey*, scale 1:100,000, 1 sheet.

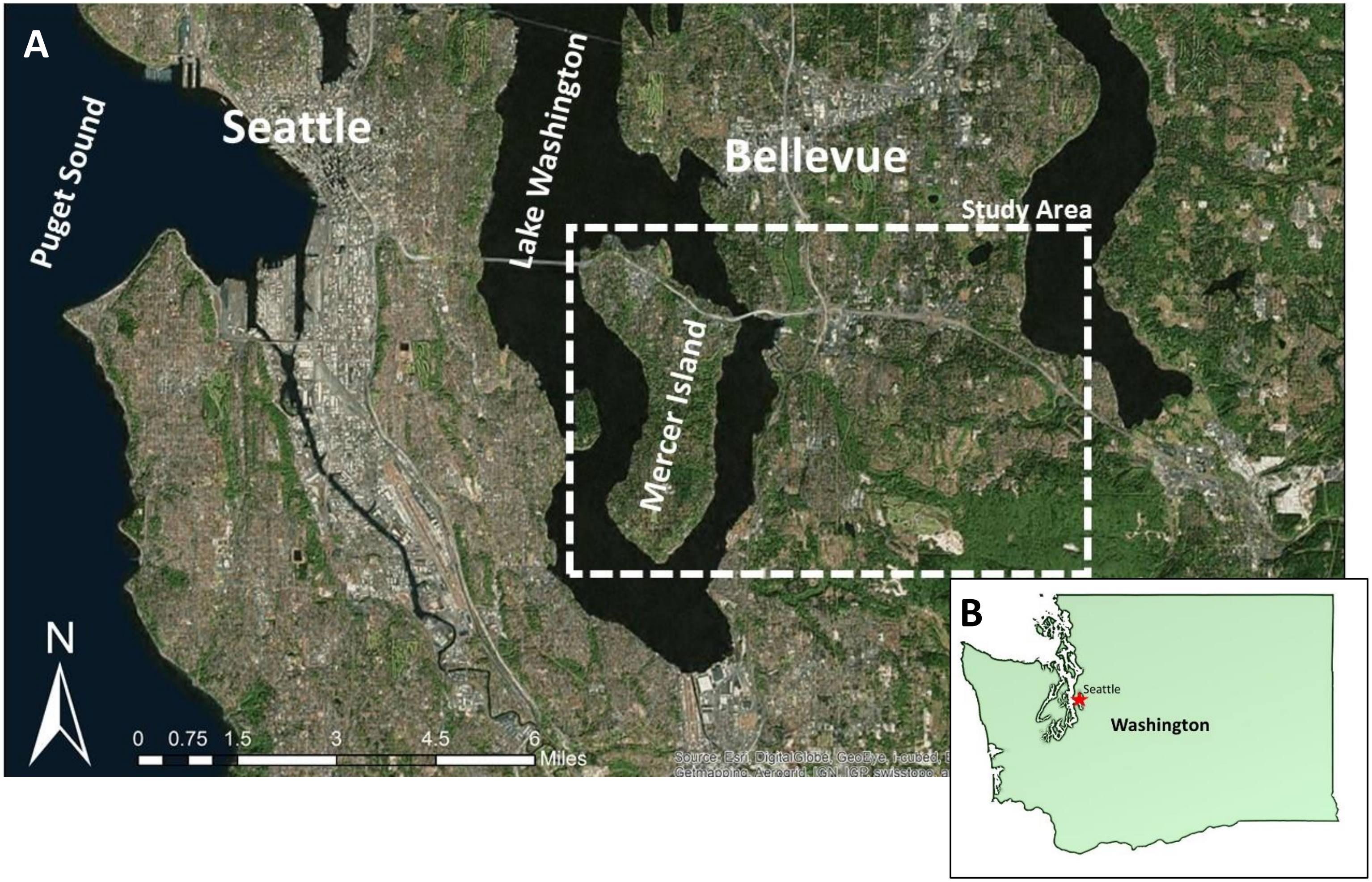

Figure 1: (A) Aerial Imagery of the Greater Seattle area. (B) Location of the study area in the Puget Lowland of Washington State.
Basemap Source: Esri, DigitalGlobe, GeoEye, i-cubed, Earthstar Geographics, CNES/Airbus DS, USDA, USGS, AEX, Getmapping, Aerogrid, IGN, IGP, swisstopo, and the GIS User Community

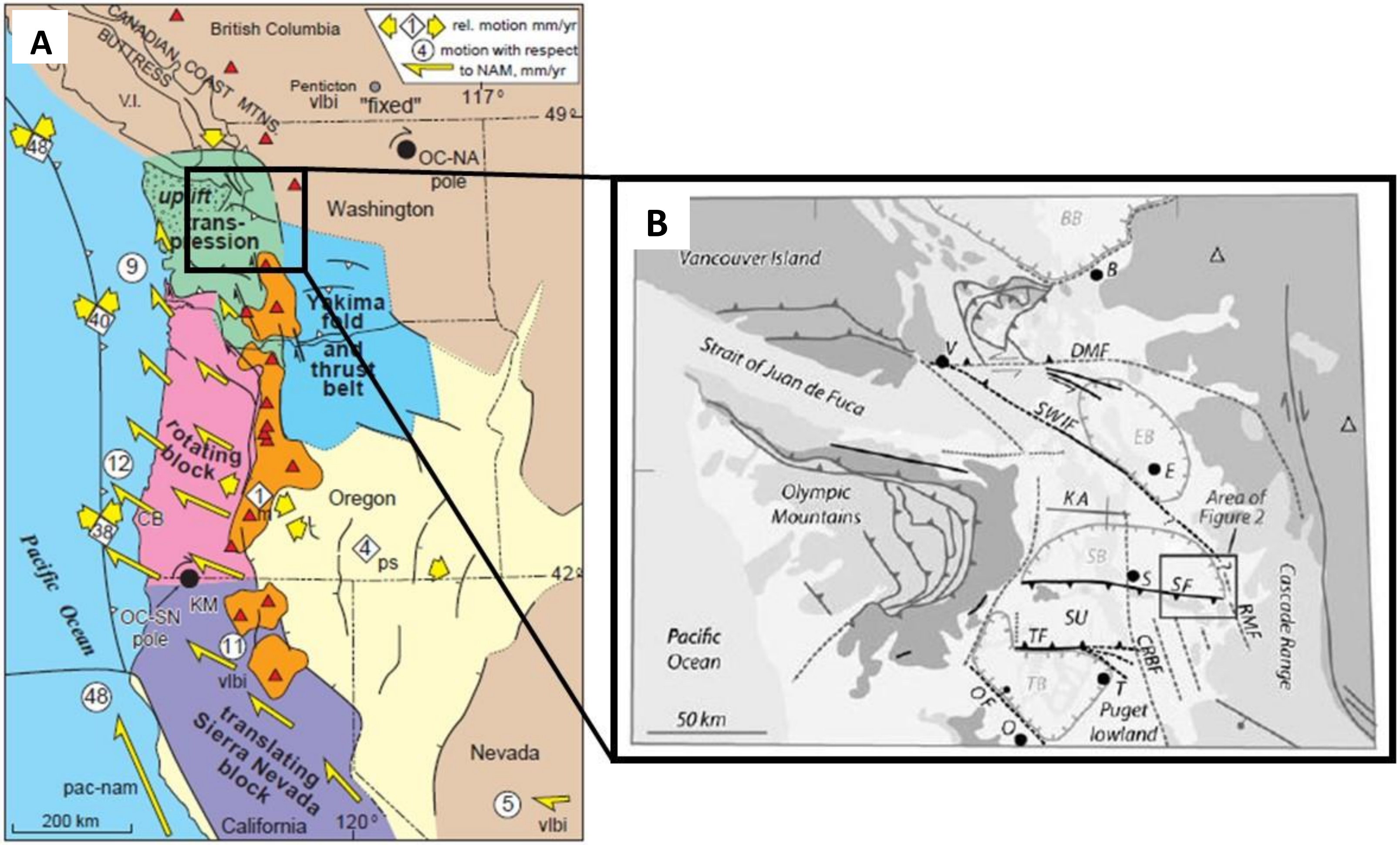

Figure 2: (A) Velocity field for Cascadia fore arc. North end of Oregon block deforms Washington fore arc against Canadian buttress, causing north-south compression, uplift, thrust faulting, and earthquakes (from Wells et al., 1998). (B) Map of the Puget Lowland showing major faults, separated by depositional basins (from Liberty and Pratt, 2008).

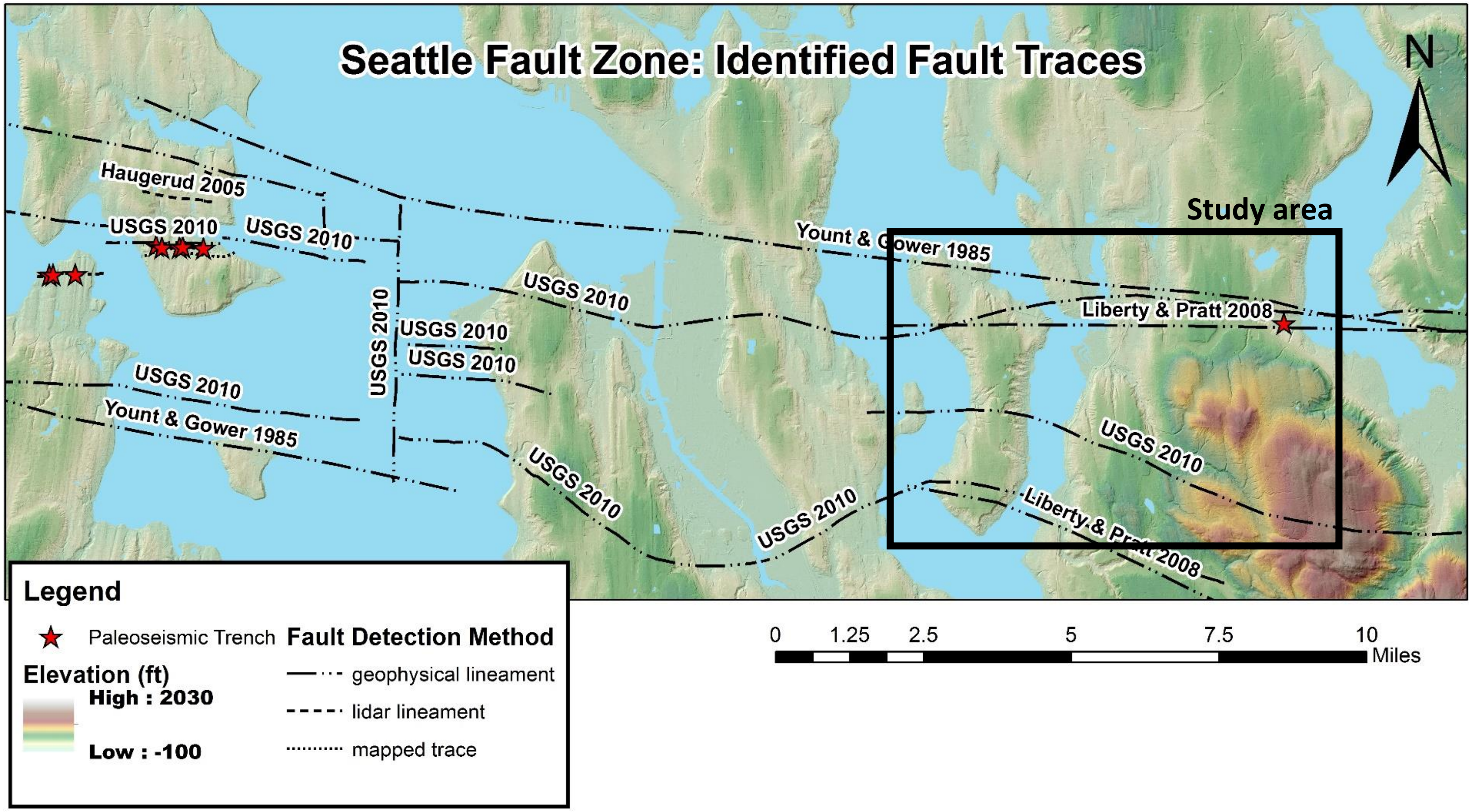

Figure 3: Map showing identified fault traces within the Seattle Fault zone. Paleoseismic trenching work has been done on Bainbridge Island in the west (Sherrod et al., 2000) and at Vasa Park in the east (Sherrod, 2002). Traces labeled "USGS 2010" were taken from the U.S. Geological Survey fold and fault database (http://earthquake.usgs.gov/hazards/qfaults/). LiDAR imagery is from the Puget Sound LiDAR Consortium.

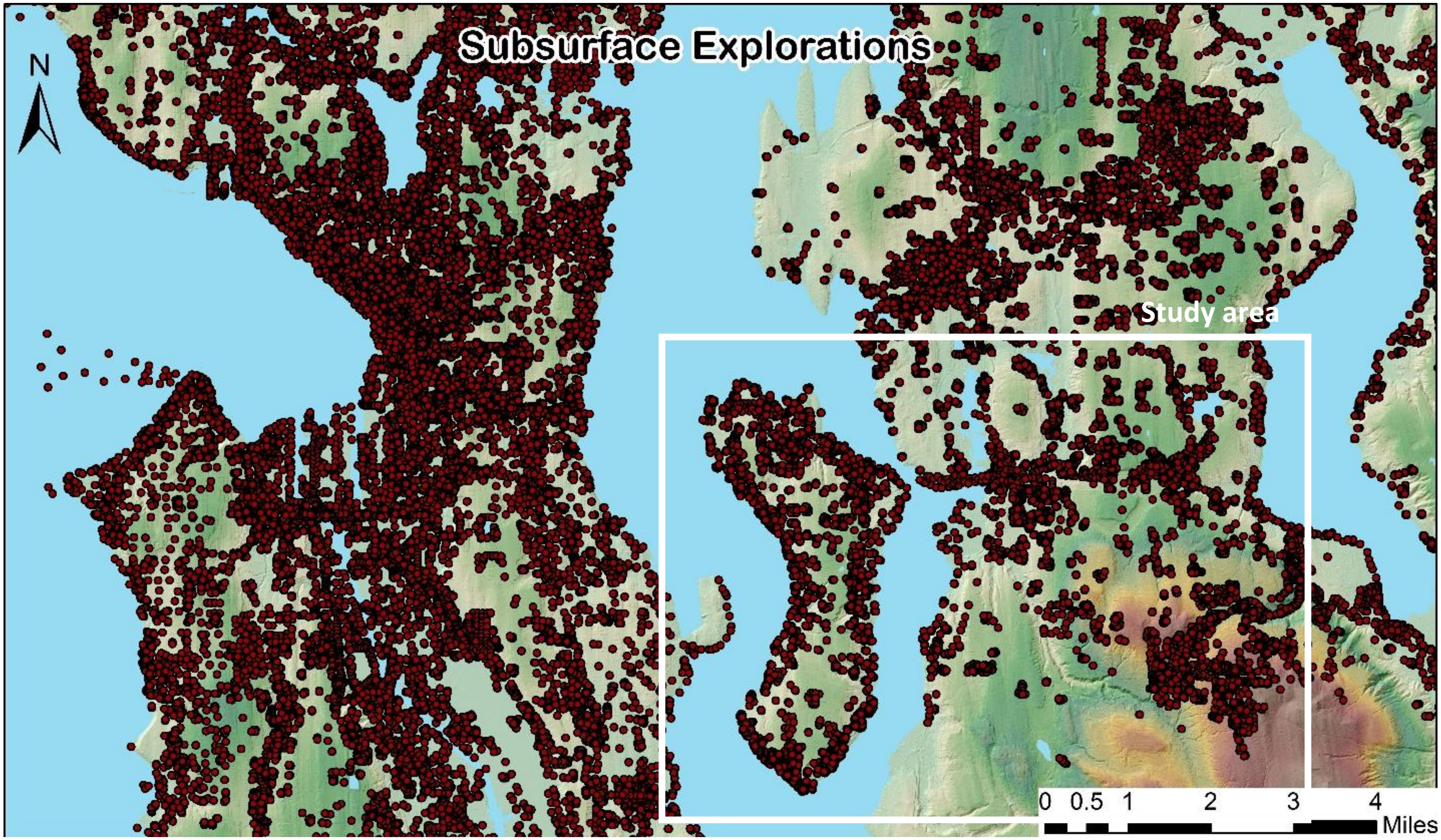

Figure 4: Map showing geotechnical explorations of the subsurface in the Greater Seattle area (courtesy of GeoMapNW).

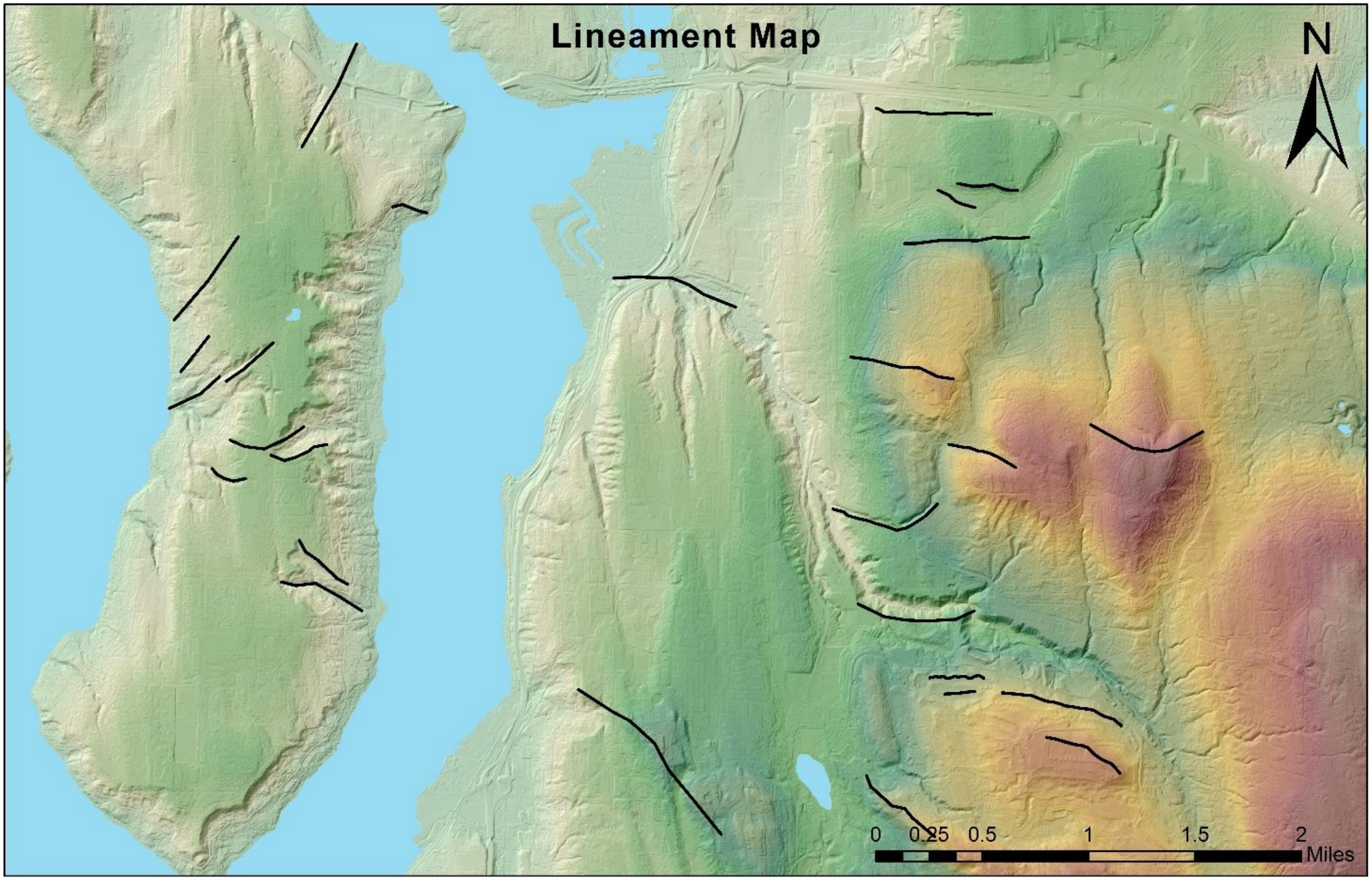

Figure 5: Map showing identified lineaments within the study area. Many of these lineaments follow or coincide with modern stream channels. Reference elevation color bar in Figure 3.

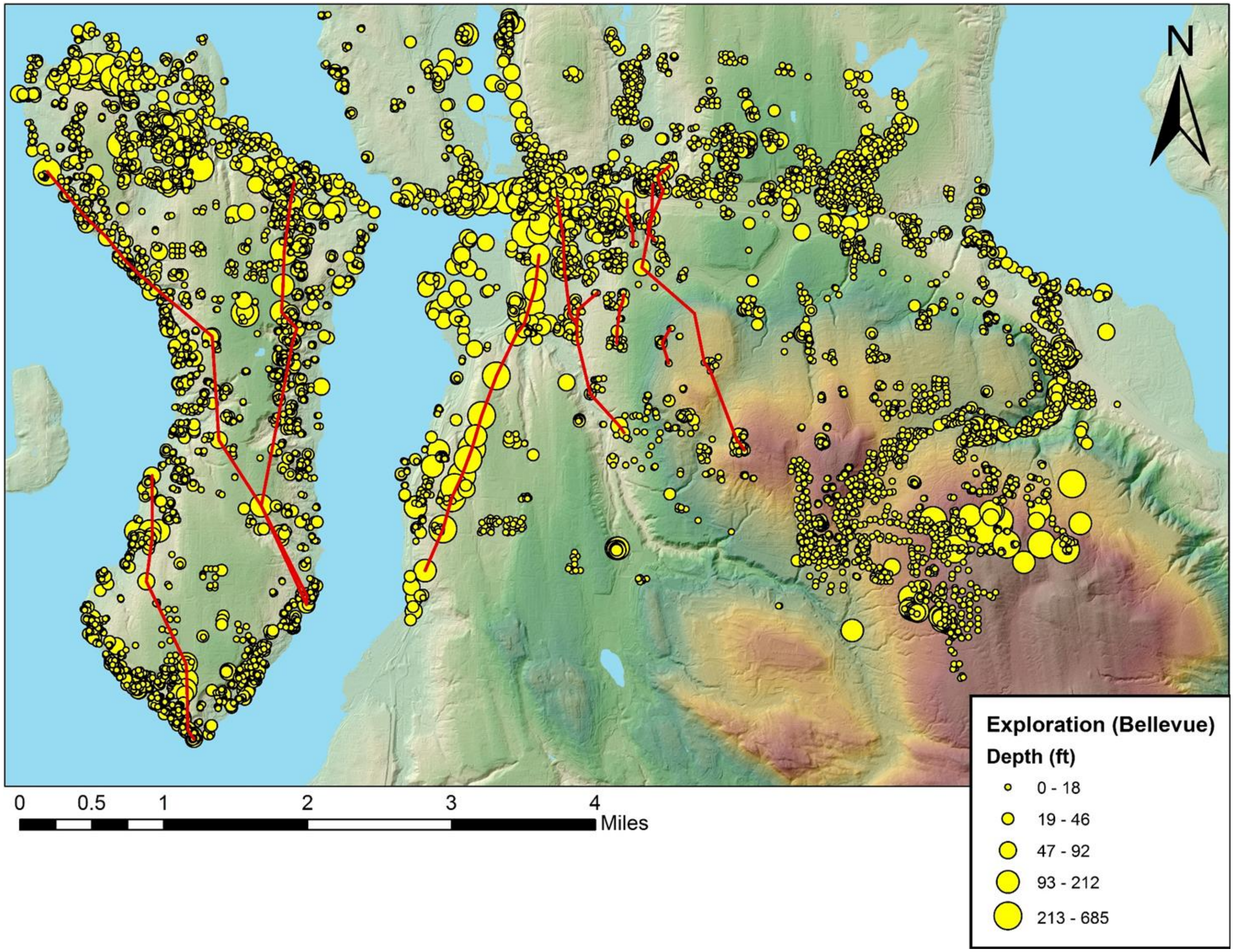

Figure 6: Map showing geotechnical subsurface explorations in the study area (GeoMapNW, http://geomapnw.ess.washington.edu/), symbolized to portray total depth of exploration. Borehole transects are shown as red lines. Reference elevation color bar in Figure 3.

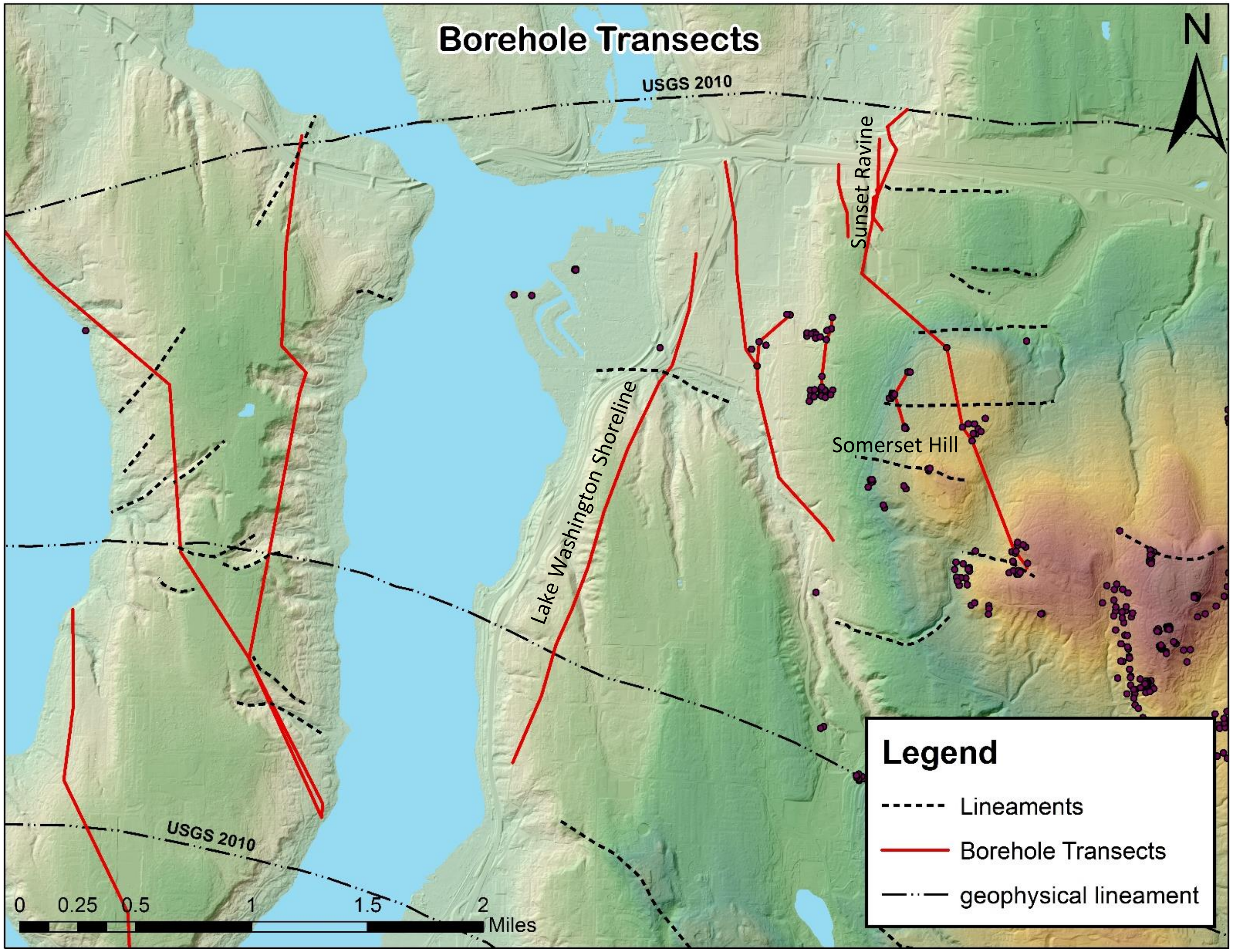

Figure 7: Map showing borehole transects analyzed using RockWorks, as well as lineaments identified in this study (dash) and lineaments identified by USGS geophysical surveys (dot-dash)

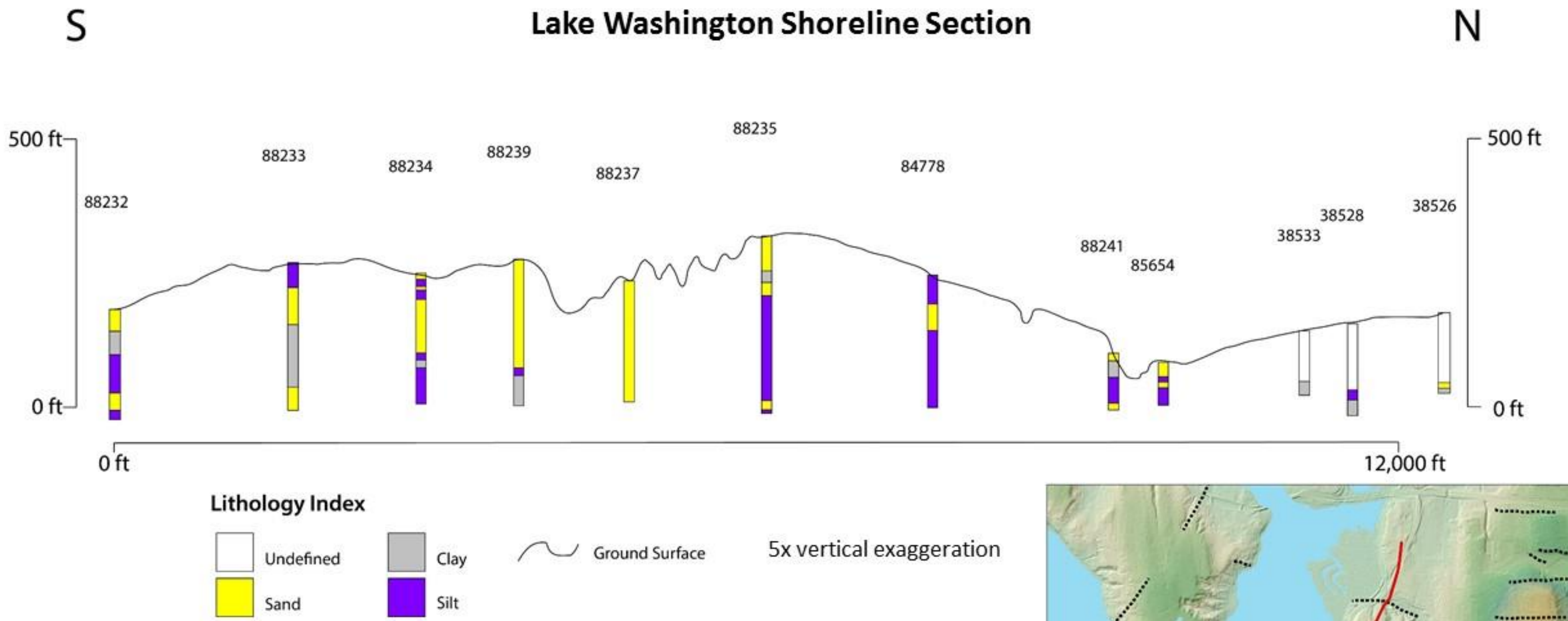

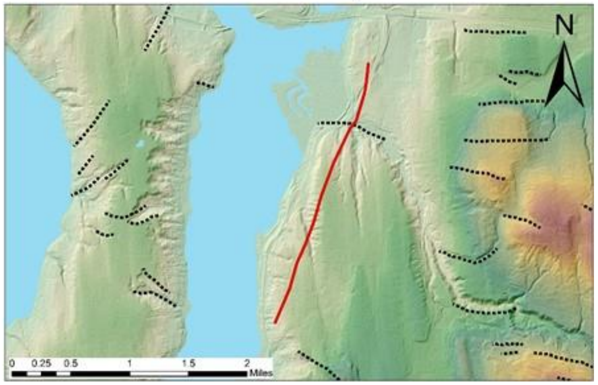

Figure 8: Strip log section created from borings near the Lake Washington shoreline.

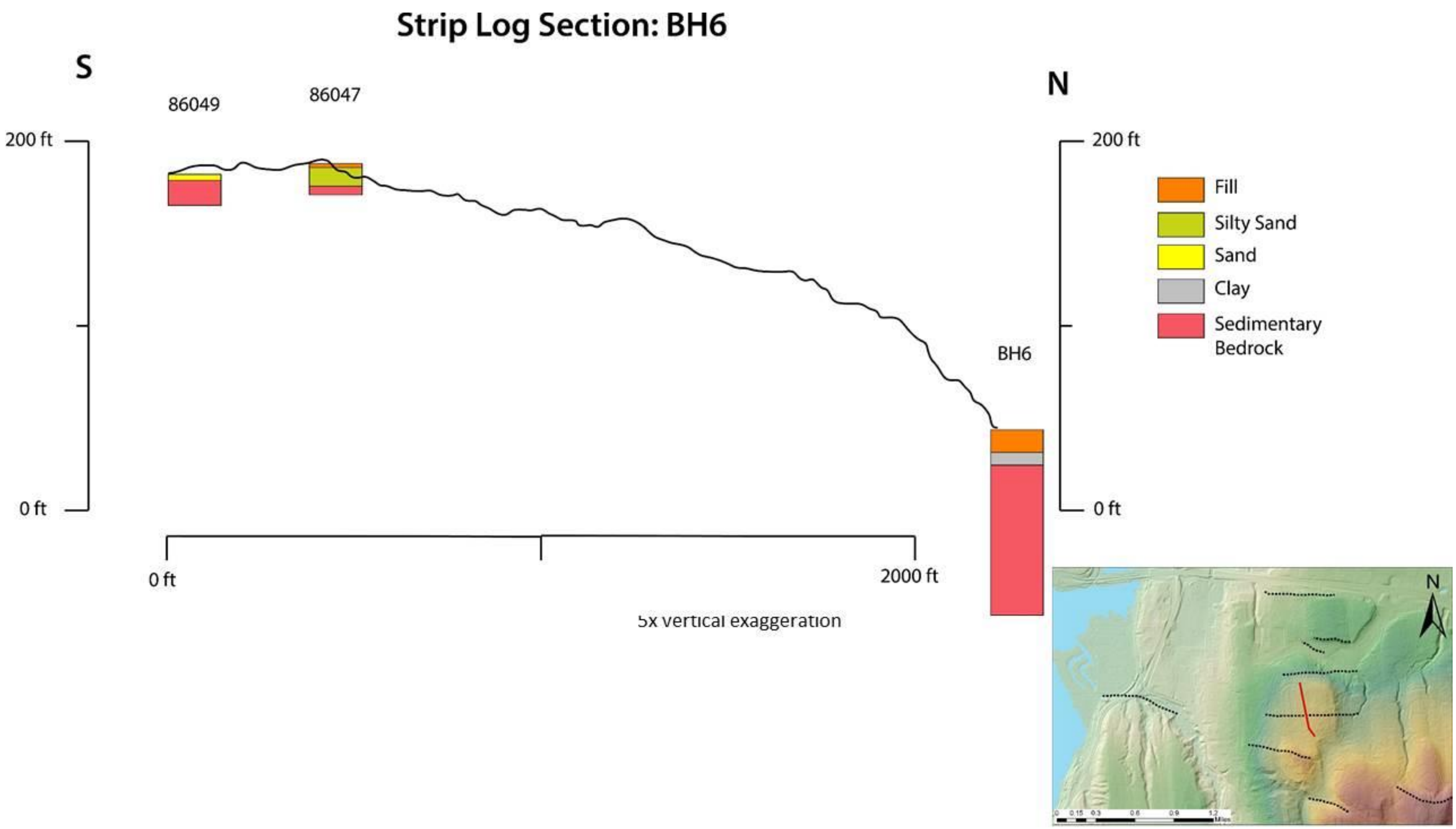

Figure 9: Strip log section created from Jacobs Associates BH-6 boring and two other nearby borings on Somerset Hill, Bellevue, WA.

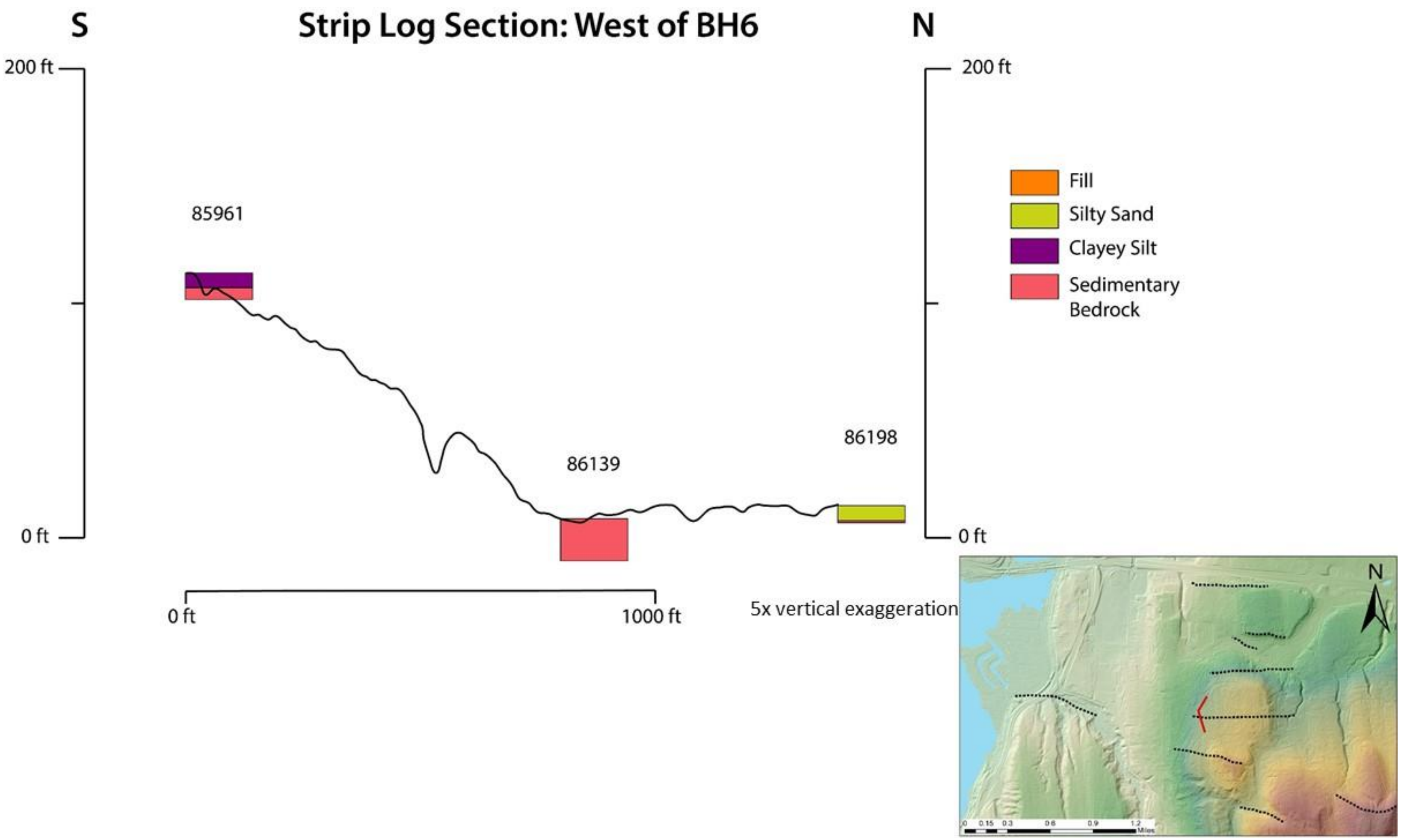

Figure 10: Strip log section created from three borings on the west slope of Somerset Hill.

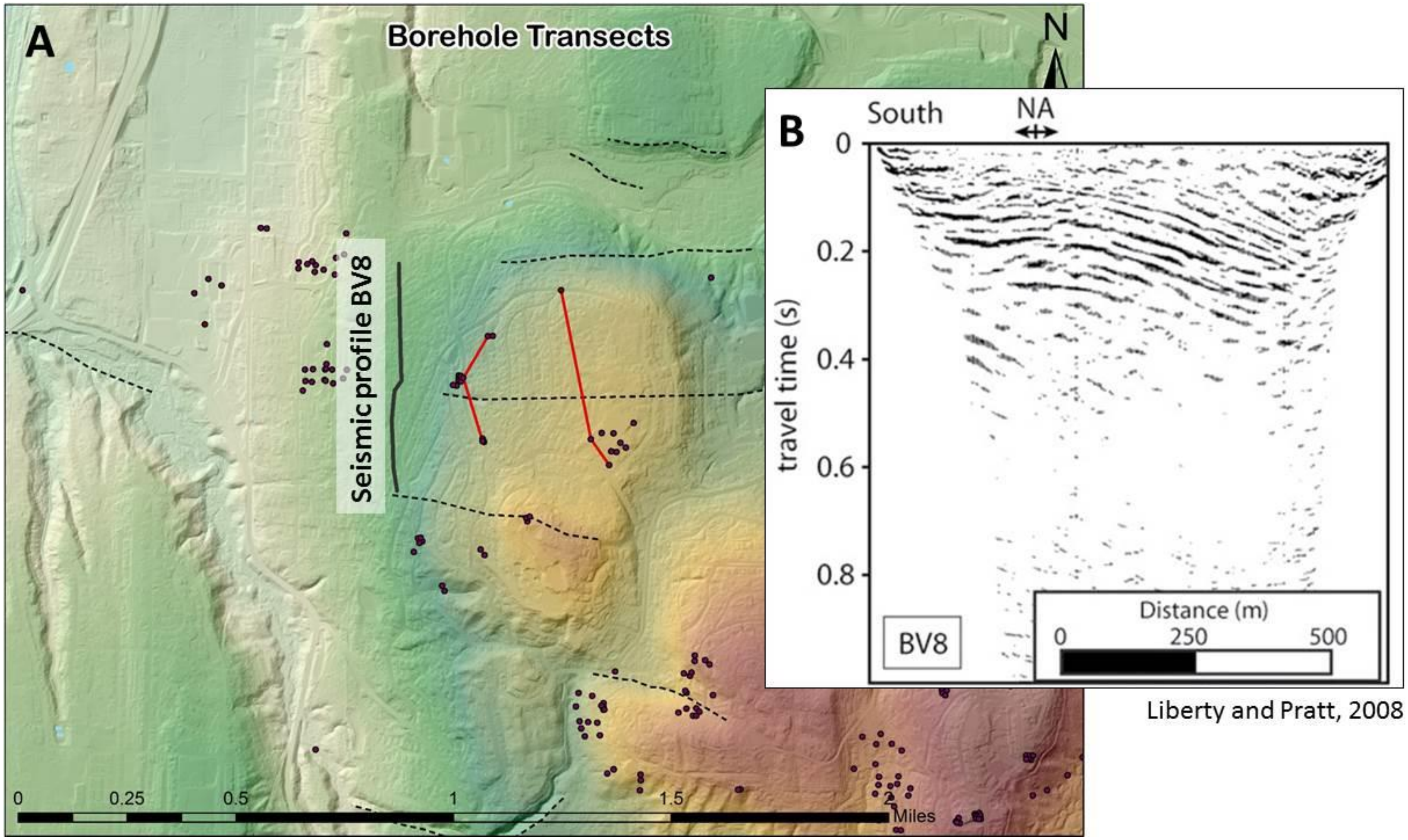

Figure 11: (A) Map showing the borehole transects on Somerset Hill in red and the seismic profile line in black. (B) Seismic profile showing predominantly north-dipping strata (from Liberty and Pratt, 2008).

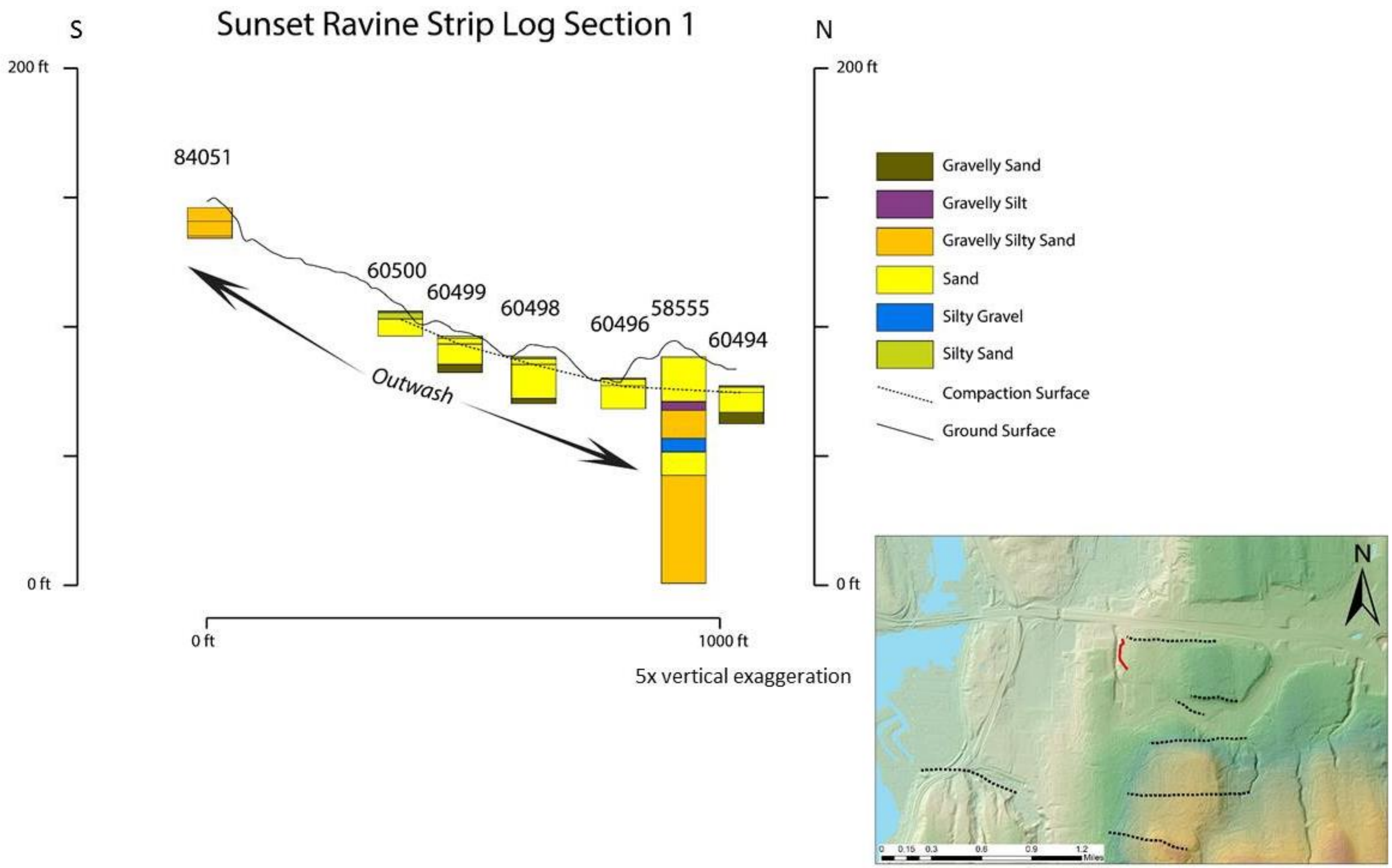

Figure 11: Strip log section created from shallow borings and test pits on the east crest of Sunset Ravine, Bellevue, WA.

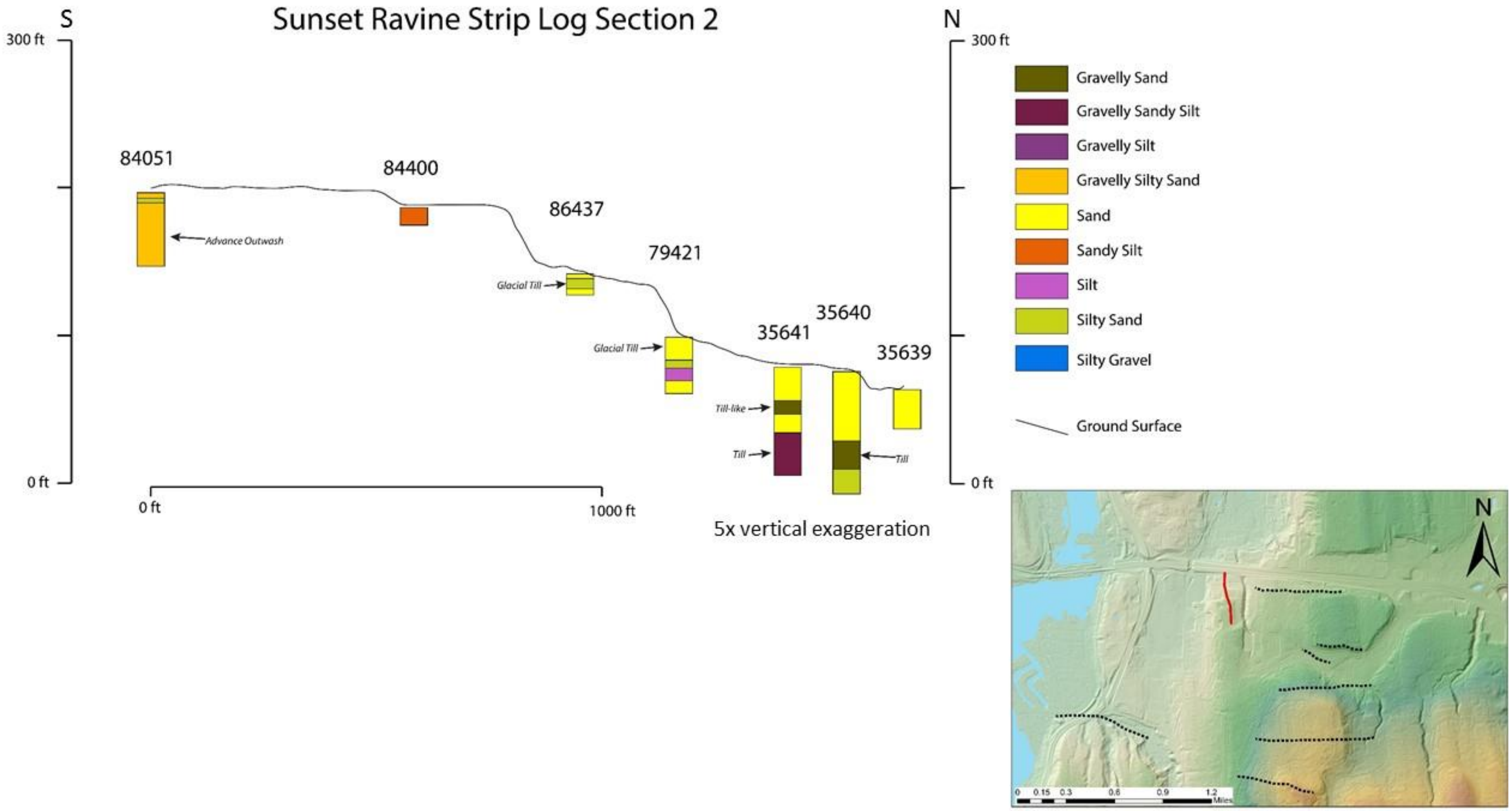

Figure 12: Strip log section created from shallow borings and test pits, less than half of a mile west of Sunset Ravine, Bellevue, WA.

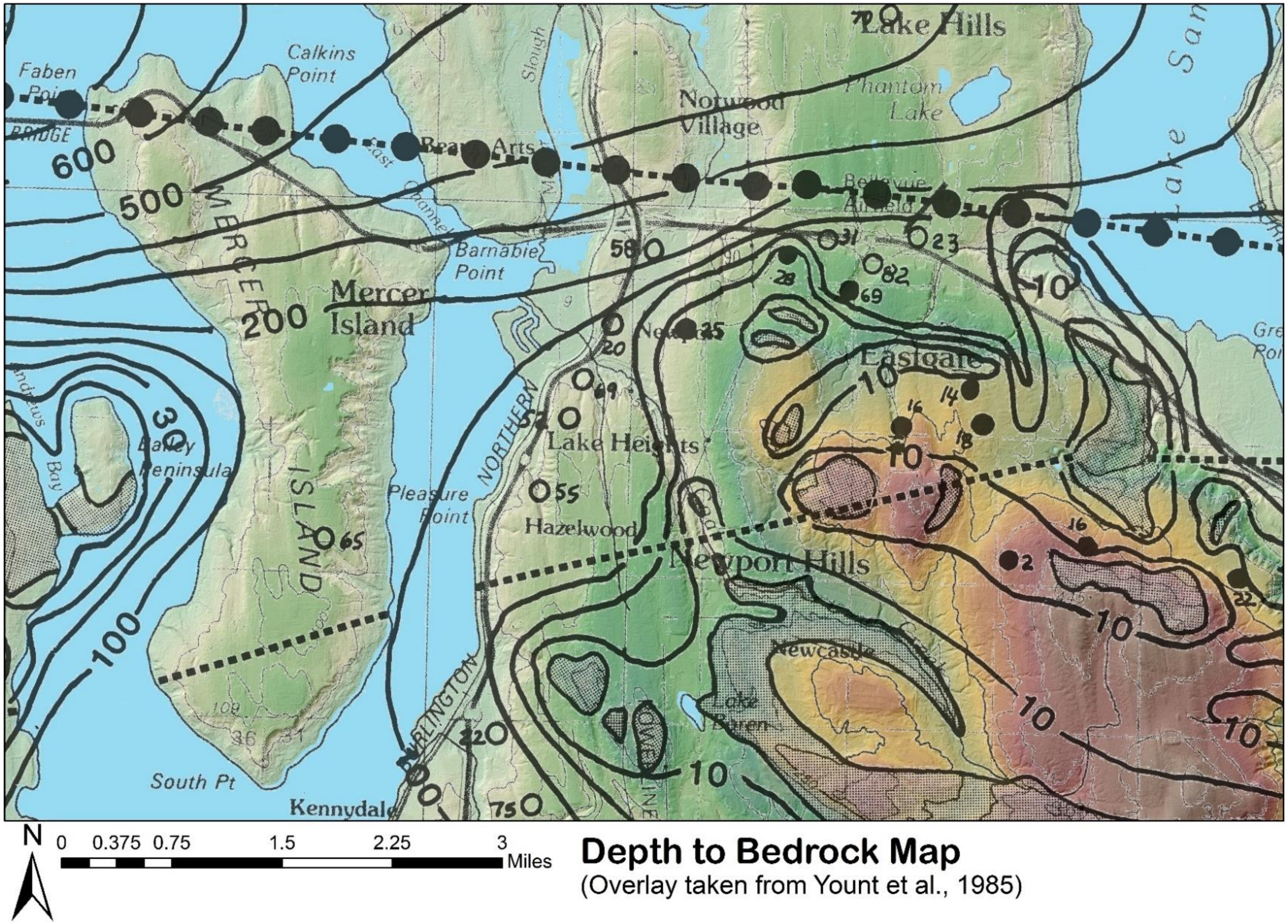

Figure 13: Map data taken from Yount et al. (1985) overlaying the study area. Shaded areas represent mapped bedrock, closed circles are water wells that intercept bedrock, open circles are water wells that do not reach bedrock, dot-dash lines are geophysical lineaments, and solid lines are contours displaying approximate depth to bedrock (in meters).

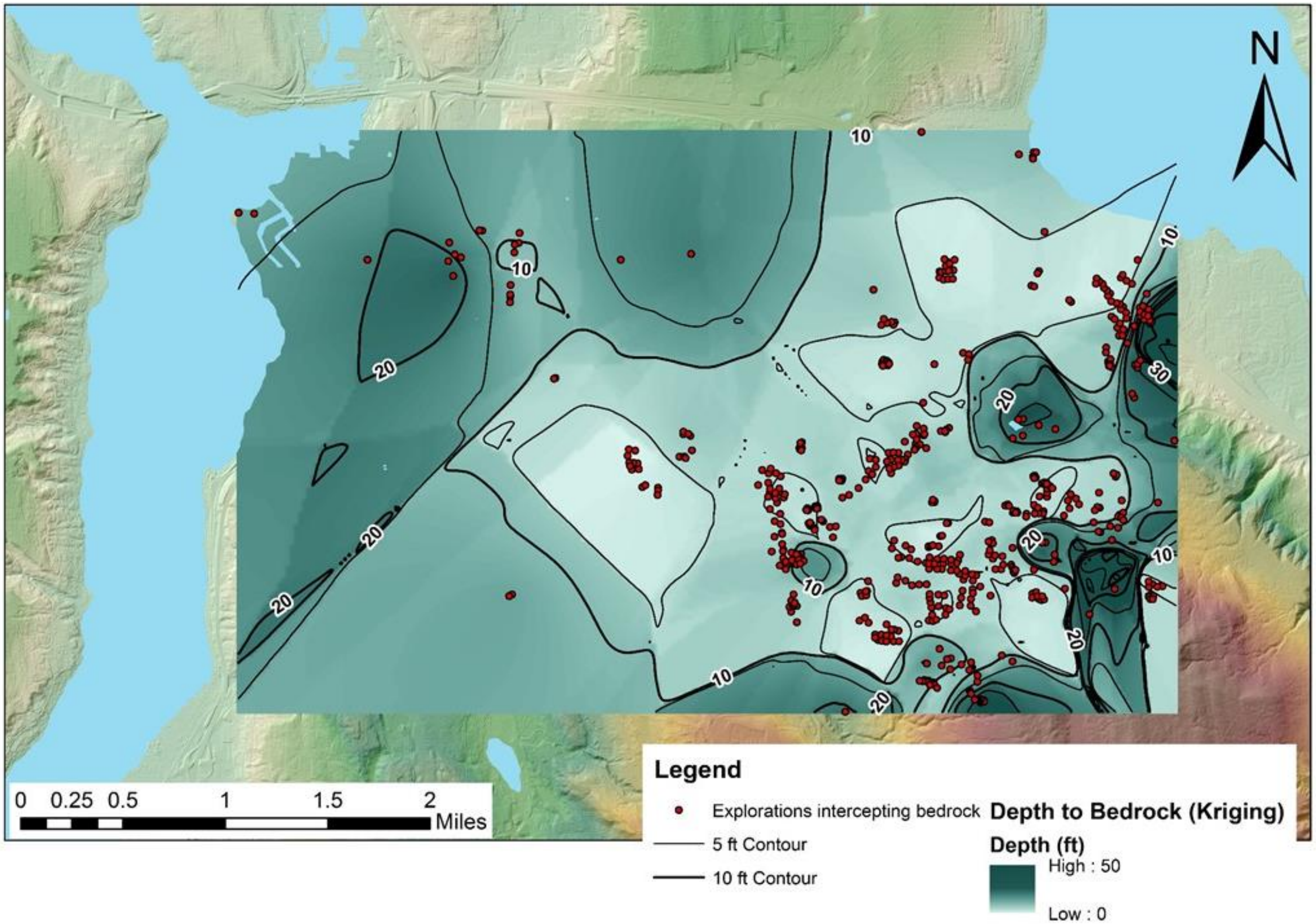

Figure 14: Depth-to-bedrock map of the study area, created from an interpolation of borings containing logged bedrock layers. Bedrock borings used in the interpolation are shown as red dots.

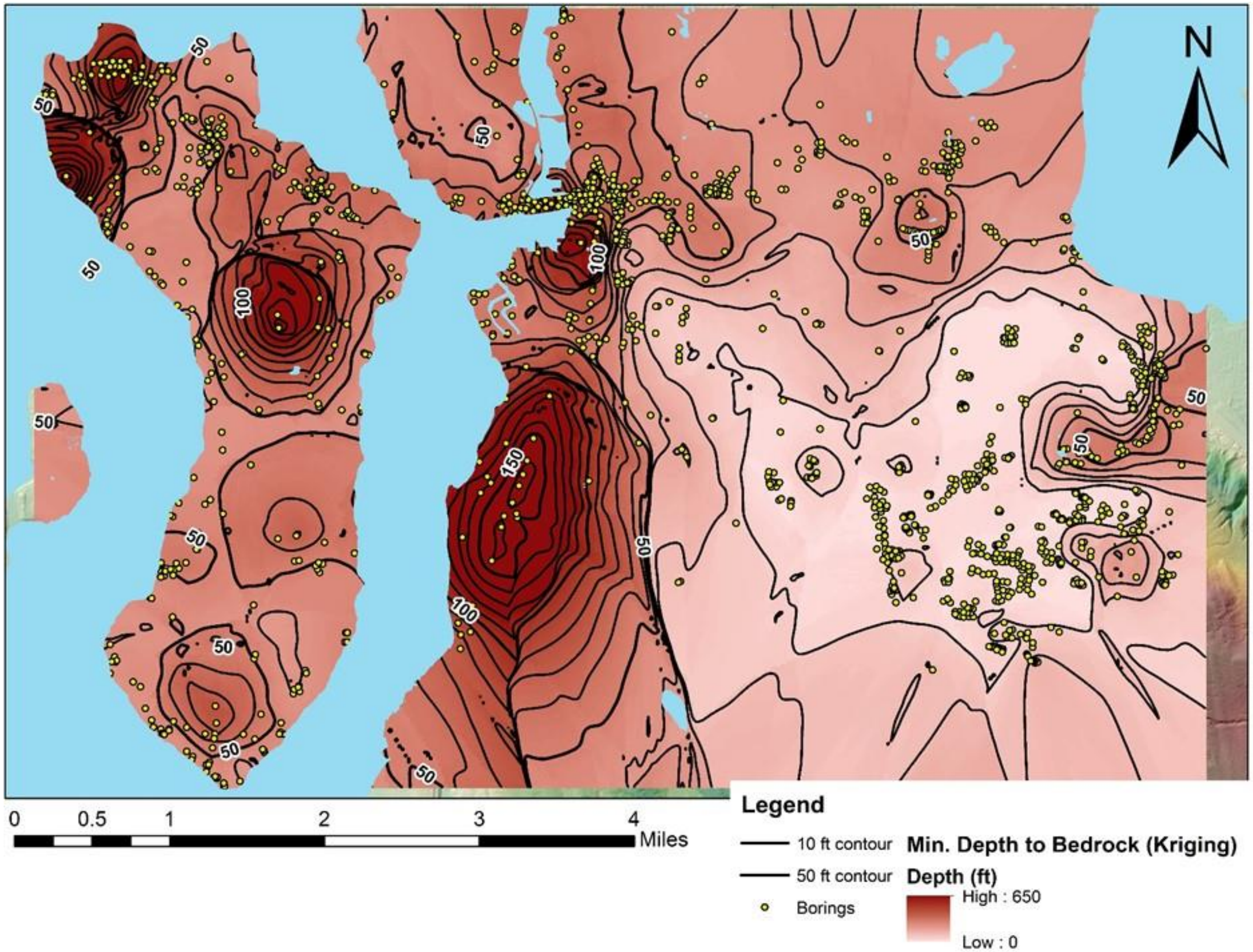

Figure 15: Map displaying minimum-depth-to-bedrock in the study area. Borings are displayed as yellow dots. Contour interval = 10 feet.

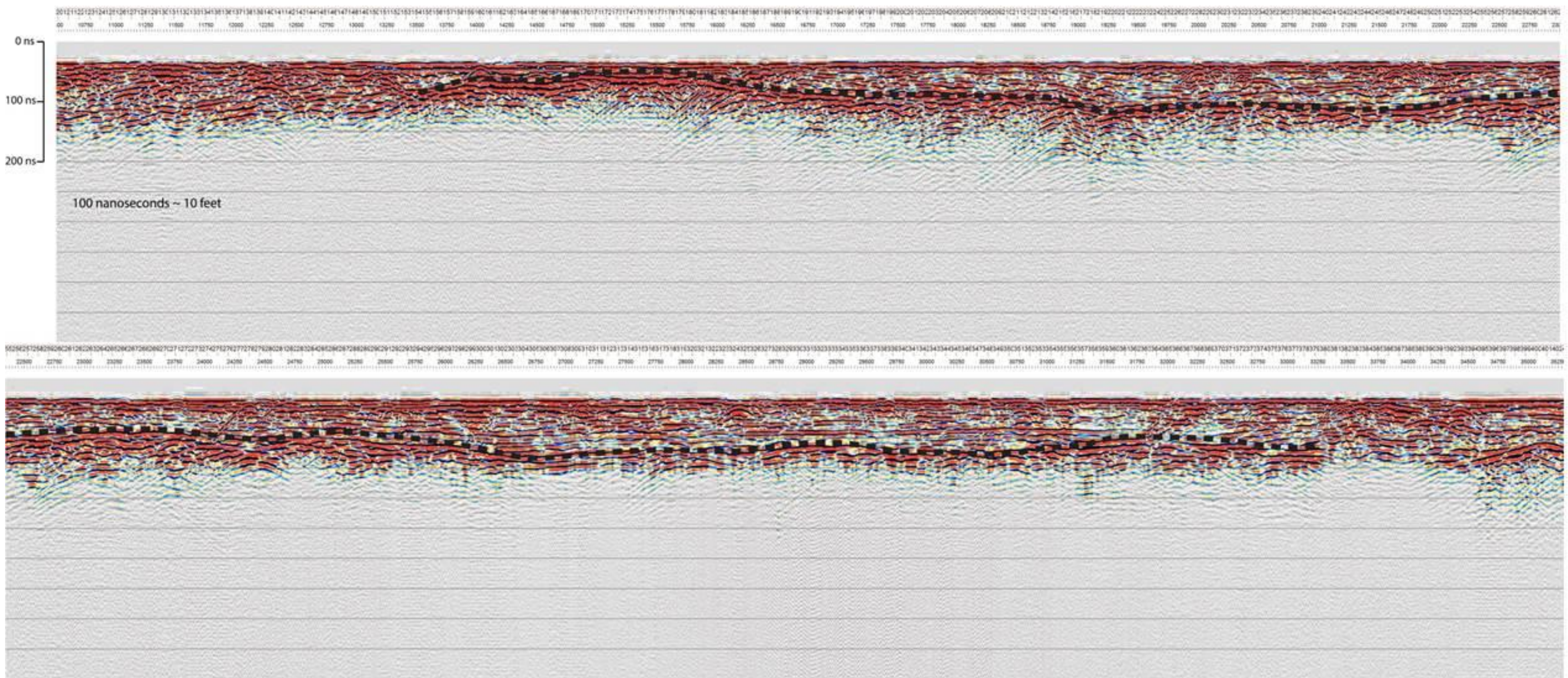

Figure 16: Ground-penetrating survey profile at Sunset Ravine. Black dashed line indicates location of the planar reflector.

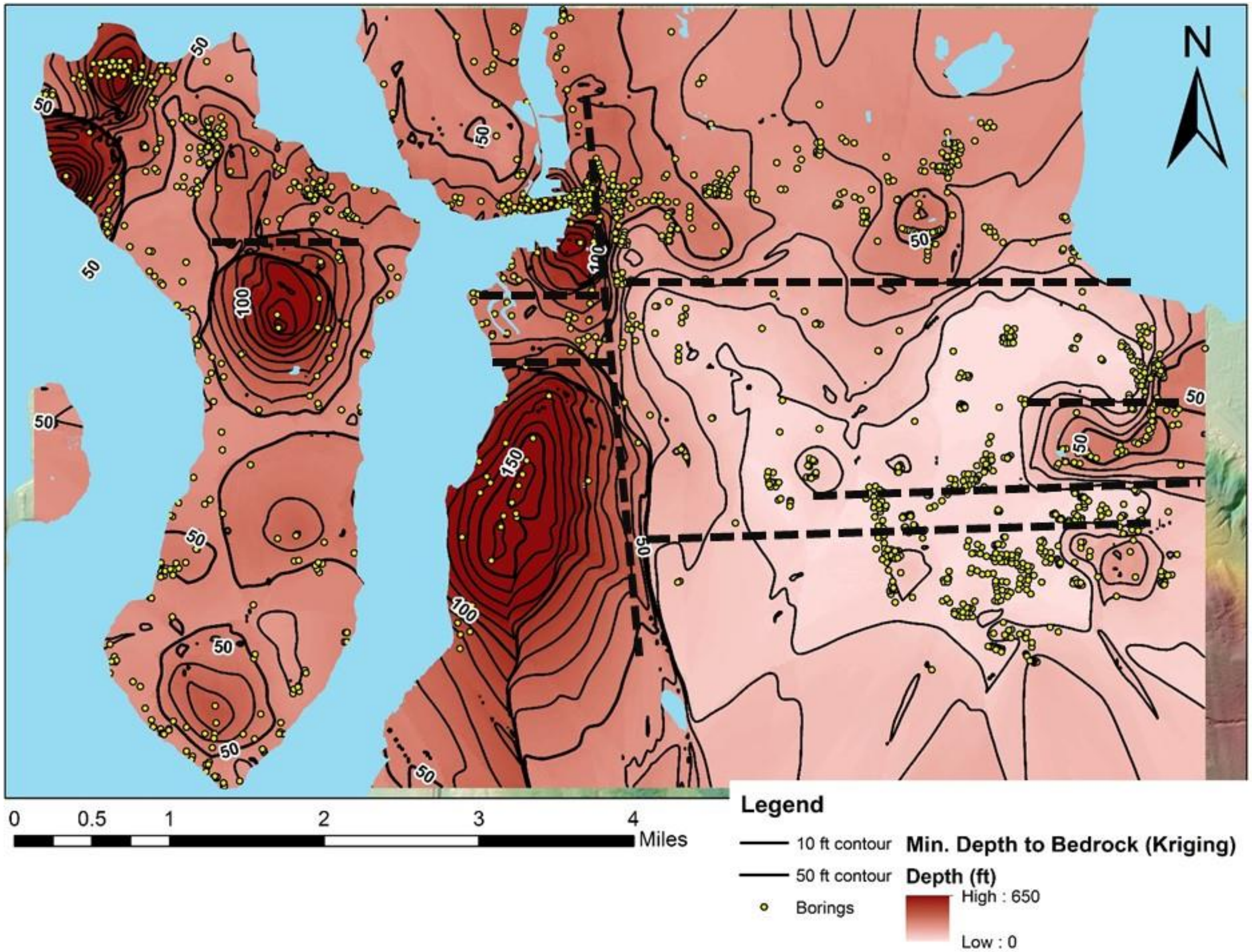

Figure 17: Map showing minimum depth to bedrock in the study area, with dashed lines portraying lineaments identified in the map.

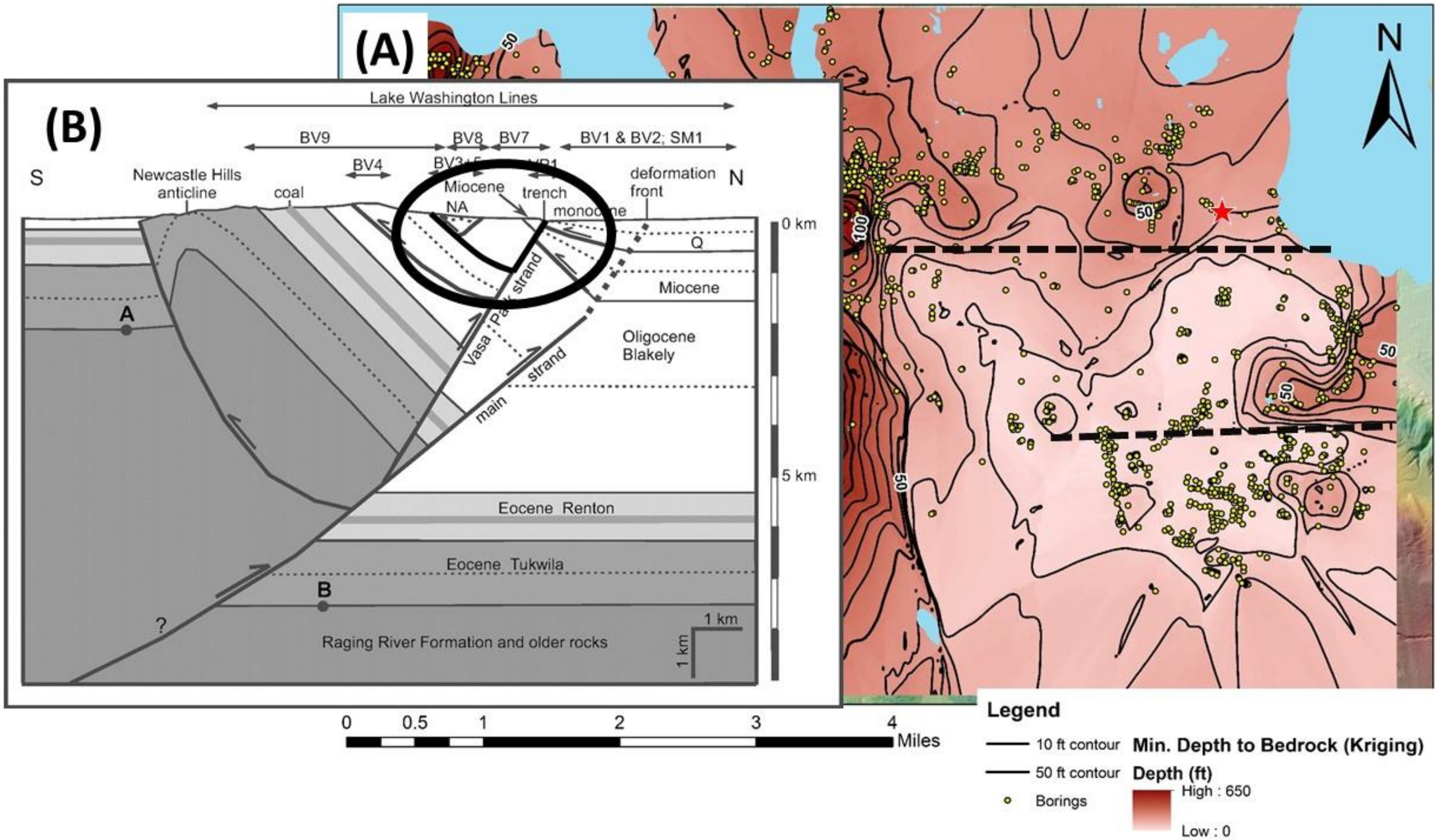

Figure 18: (A) Map showing minimum depth to bedrock in the study area and two of the identified east-west trending lineaments. (B) Interpreted structure of the fault zone underlying Bellevue, WA (from Liberty and Pratt, 2008). Uplifted block representing the area bounded by the two identified east-west lineaments in (A) is circled. The Vasa Park Trench site is represented by the red star.

TABLES

Table 1: Summary of major material logged in all subsurface layers within the study area

Material Major	**Bellevue Count**
Asphalt/Concrete	424
Clay	995
Cobbles	9
Gravel	827
No Description	69
Peat	201
Plutonic Rock	1
Sedimentary Rock	680
Volcanic Rock	3
Sand	5643
Silt	3233
Topsoil/Vegetation	2538
Unknown	252

Table 2: Summary of relevant exploration types in the study area

Exploration Type	**Bellevue Count**
Boring	3064
CPT (cone penetration)	19
Exposure	19
Test Pit	3945
Well	142